Inorganic Chemistry

Article

pubs.acs.org/IC

Physicochemical Analysis of Ruthenium(II) Sensitizers of 1,2,3-Triazole-Derived Mesoionic Carbene and Cyclometalating Ligands

Stephan Sinn,[†,§] Benjamin Schulze,[†,§] Christian Friebe,[†,§] Douglas G. Brown,[‡] Michael Jäger,[†,§] Esra Altuntaş,[†,§] Joachim Kübel,[#,⊥] Oliver Guntner,[#] Curtis P. Berlinguette,*[,‡,∥] Benjamin Dietzek,*[,#,⊥,§] and Ulrich S. Schubert*[,†,§]

[†]Laboratory of Organic and Macromolecular Chemistry (IOMC), Friedrich Schiller University Jena, Humboldtstr. 10, 07743 Jena, Germany

[§]Jena Center for Soft Matter (JCSM), Friedrich Schiller University Jena, Philosophenweg 7, 07743 Jena, Germany

[‡]Department of Chemistry, University of Calgary, 2500 University Drive N.W., Calgary, Alberta, Canada T2N 1N4

[∥]Department of Chemistry, The University of British Columbia, 2036 Main Mall, Vancouver, British Columbia, Canada V6T 1Z1

[#]Institute of Physical Chemistry (IPC) and Abbe Center of Photonics, Friedrich Schiller University Jena, Helmholtzweg 4, 07743 Jena, Germany

[⊥]Leibniz Institute of Photonic Technology (IPHT), Albert-Einstein-Str. 9, 07745 Jena, Germany

Supporting Information

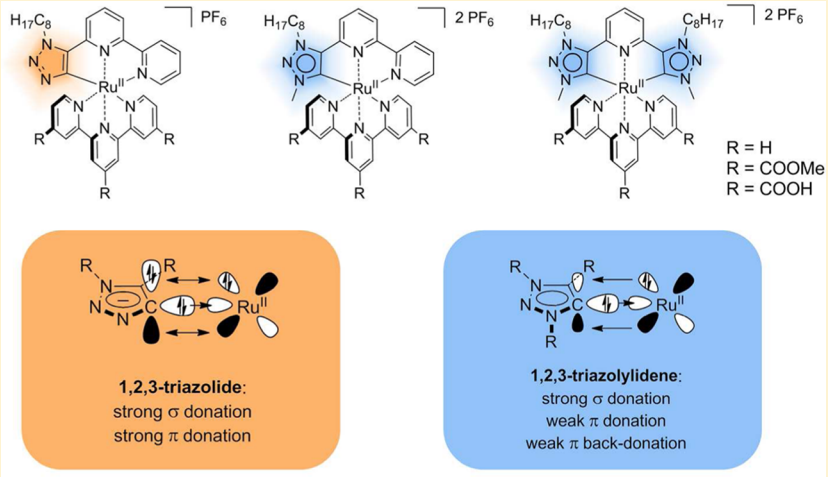

ABSTRACT: A series of heteroleptic bis(tridentate) ruthenium(II) complexes bearing ligands featuring 1,2,3-triazolide and 1,2,3-triazolylidene units are presented. The synthesis of the C^N^N-coordinated ruthenium(II) triazolide complex is achieved by direct C−H activation, which is enabled by the use of a 1,5-disubstituted triazole. By postcomplexation alkylation, the ruthenium(II) 1,2,3-triazolide complex can be converted to the corresponding 1,2,3-triazolylidene complex. Additionally, a ruthenium(II) complex featuring a C^N^C-coordinating bis(1,2,3-triazolylidene)pyridine ligand is prepared via transmetalation from a silver(I) triazolylidene precursor. The electronic consequences of the carbanion and mesoionic carbene donors are studied both experimentally and computationally. The presented complexes exhibit a broad absorption in the visible region as well as long lifetimes of the charge-separated excited state suggesting their application in photoredox catalysis and photovoltaics. Testing of the dyes in a conventional dye-sensitized solar cell (DSSC) generates, however, only modest power conversion efficiencies (PCEs).

INTRODUCTION

Ruthenium(II) polypyridyl complexes are promising candidates for the utilization of solar energy by means of photoredox catalysis,[1−5] artificial photosynthesis,[6] and photovoltaic applications like dye-sensitized solar cells (DSSCs),[7−9] as they allow for a light-driven charge separation by a metal-to-ligand charge transfer (MLCT).[10] To exploit the charge-separated triplet excited state (^{3}MLCT), photo- and redox-stability as well as sufficiently long excited-state lifetimes are required. Bis(tridentate) ruthenium(II) complexes, e.g., $[Ru(tpy)_2]^{2+}$ (tpy = 2,2′:6′,2″-terpyridine), offer a high stability and allow for isomer-free functionalization, but usually suffer from short-lived excited states owing to a rapid deactivation via an energetically

Received: October 27, 2013
Published: January 28, 2014

   dx.doi.org/10.1021/ic402702z | Inorg. Chem. 2014, 53, 2083−2095

low lying triplet metal-centered excited state (^{3}MC). The latter is caused by the nonideal bite angle of the tpy ligand, which weakens the σ donation from the outer pyridine rings and, therefore, lowers the energy of the corresponding σ-antibonding orbitals, which are mainly of $d_{x^2-y^2}$ character.[11,12] Different strategies have been developed during the past decades to overcome the poor photophysical properties that are typical for $[Ru(tpy)_2]^{2+}$ including structural[13] and electronic[14,15] manipulations. The latter usually involve an increase of the σ-donor strength by introducing, for instance, carbanionic or carbene donors in the peripheral positions of the tridentate ligand, which help to destabilize the ^{3}MC. Additionally, a decelerated radiationless deactivation of the ^{3}MLCT via the ^{3}MC in organometallic ruthenium(II) complexes may be caused not only by a higher energy barrier, but also by a lower pre-exponential factor.[16,17]

When comparing the electronic effects of carbanion and carbene donors, the repulsive d(π)−p(π) interaction between the metal center and the carbanion raises the energy of the ^{3}MLCT and, to a greater extent, that of the ground state (GS) resulting in a small ^{3}MLCT−^{3}MC energy gap. The latter enables efficient light harvesting in the DSSC,[7,18] but shortens the excited-state lifetimes by virtue of the energy-gap law.[11,19−23] Additionally, as the ^{3}MLCT is destabilized, the ^{3}MLCT−^{3}MC energy separation is lowered, which facilitates the nonradiative deactivation via the ^{3}MC. In contrast, charge-neutral *N*-heterocyclic carbenes (NHCs) like imidazol-2-ylidenes and mesoionic carbenes (MICs) such as 1,2,3-triazolylidenes allow for significant ^{3}MC destabilization, while the GS and ^{3}MLCT energies are less affected, which results in significantly prolonged excited-state lifetimes.[24] Recently, we could demonstrate that the exploitation of the superior σ donation provided by 1,2,3-triazolylidenes allows for the design of bis(tridentate) ruthenium(II) complexes with excited-state lifetimes of up to several microseconds.[25−27]

In this work, we present the photophysical and electrochemical properties of a series of heteroleptic bis(tridentate) ruthenium(II) complexes of 1,2,3-triazole-derived ligands that involve either anionic 1,2,3-triazolide or mesoionic 1,2,3-triazolylidene donors (Figure 1).[28] Relative to the *N*-coordination of the triazole via its 3-nitrogen, the *C*-coordination of the triazolide or triazolylidene enables significantly stronger σ donation.[29,30] Thereby, the anionic triazolide additionally acts as a π donor, owing to the high energy of the π system. In contrast, the π and π^* orbitals of the mesoionic 1,2,3-triazolylidene are lower in energy resulting in a weakened π donation and strengthened π back-donation (Figure 2).[25] Beside the fundamental properties, we were interested in the viability of these dyes for application in the DSSC, as the long excited-state lifetimes of the mesoionic carbene complexes (**2c**, **3c**) might enable high electron injection efficiencies with a low injection driving force, i.e., with a low energy loss.[31,32] Furthermore, electron donation from phenyl anions within cyclometalated ruthenium(II) complexes can afford Ru(III)/Ru(II) redox potentials that are too low to allow for efficient dye regeneration. In these cases, the installation of electron-withdrawing groups may be necessary in order to increase the redox potential.[33,34] In this regard, we were interested in whether the intrinsically stabilized carbanion of the anionic 1,2,3-triazolide donor (**1c**) can serve as a valuable alternative.

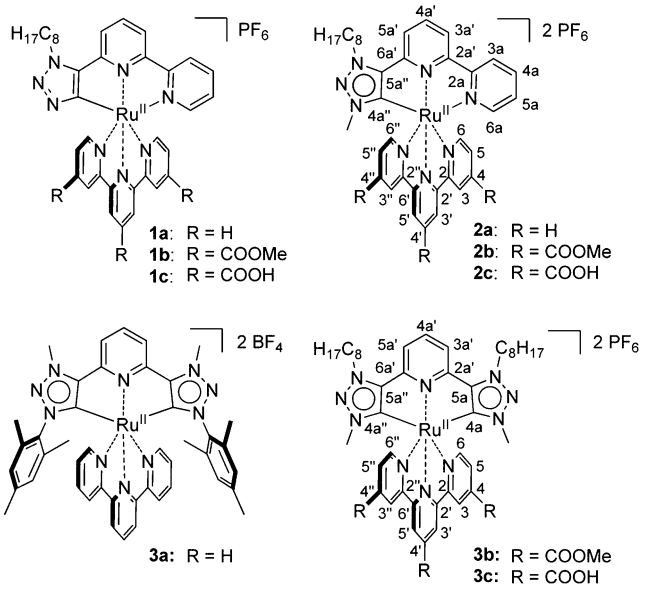

Figure 1. Ruthenium(II) complexes studied in this work. Numbering schemes for the complexes and the corresponding ligands.

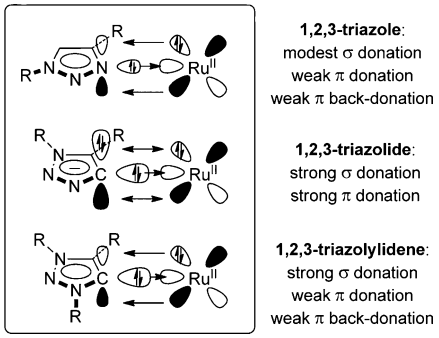

Figure 2. Illustration of the electronic differences between 1,2,3-triazolide and 1,2,3-triazolylidene donors. Note that the π donation is repulsive (cf. 1,2,3-triazolide).

1,2,3-Triazole-derived ligands can be readily synthesized and functionalized via catalyzed azide−alkyne cycloaddition reactions.[30,35,36] We chose the ruthenium-catalyzed version to selectively obtain the 1,5-disubstituted triazole.[37] In contrast to the 1,4-disubstituted triazole, the 1,5-regioisomer exclusively affords the cyclometalated complex, because the alternative tridentate coordination via the 3-nitrogen of the triazole is blocked (Figure 3).[38] Additionally, as the corresponding

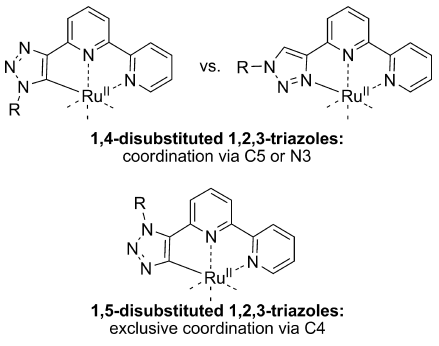

Figure 3. Implications of the ligand design for the ruthenium(II) coordination.

dx.doi.org/10.1021/ic402702z | *Inorg. Chem.* 2014, 53, 2083−2095

Scheme 1. Synthesis Routes Towards the Ruthenium(II) Complexes 1a−1c, 2a−2c, and 3a−3c[a]

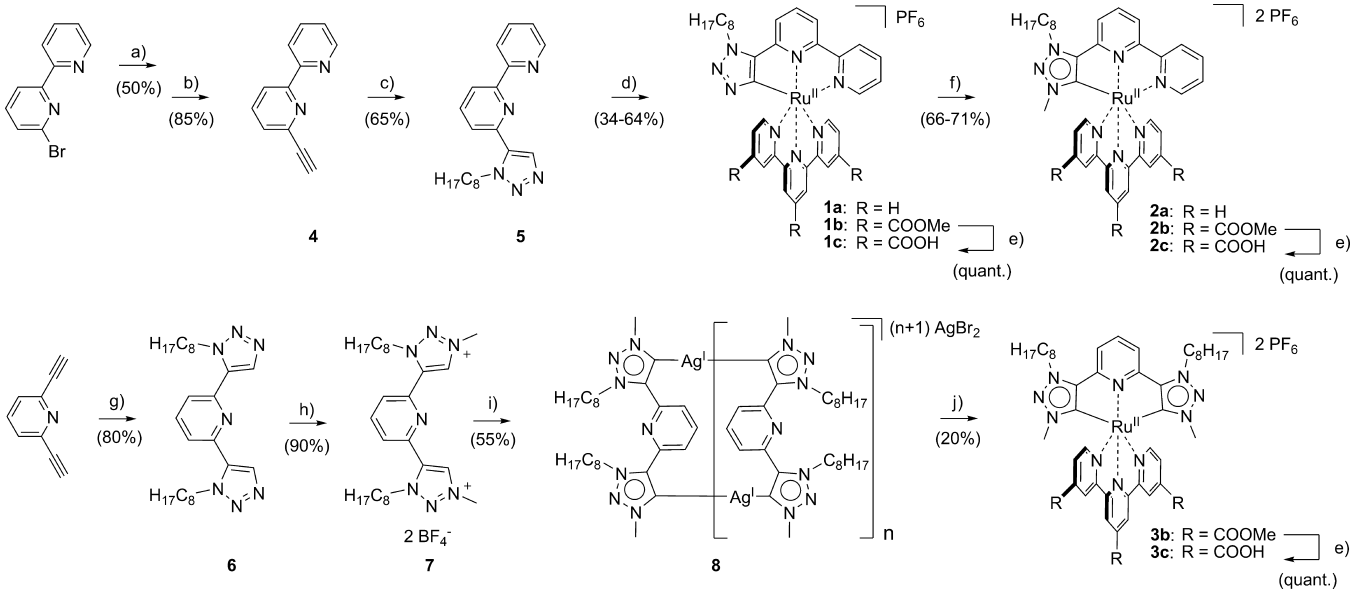

[a](a) Trimethylsilylacetylene, $Pd(PPh_3)_4$, CuI, THF, diisopropylamine, rt, 3 d; (b) KF, THF/MeOH, rt, 24 h; (c) *n*-octyl azide, $RuCp^*(PPh_3)_2Cl$, 1,4-dioxane, 60 °C, microwave, 3 h; (d) $[Ru^{II}(tpy)(MeCN)_3](PF_6)_2$ or $[Ru^{II}(tcmtpy)(MeCN)_3](PF_6)_2$, MeOH (+ 2,6-lutidine) or DMF, 160 °C, microwave, 30 min; (e) $DMF/NEt_3/H_2O$, reflux, 48 h; (f) MeI, $CHCl_3$, 70 °C, 48 h; (g) *n*-octyl azide, $RuCp^*(PPh_3)_2Cl$, 1,4-dioxane, 60 °C, microwave, 3 h; (h) $Me_3O^+BF_4^-$, CH_2Cl_2, rt, 48 h; (i) Ag_2O, KBr, MeCN, rt, 96 h; (j) $Ru(tcmtpy)(DMSO)Cl_2$, CH_2Cl_2, 70 °C, 24 h.

triazolide and triazolylidene complexes are supposed to be anchored to TiO_2 via the tpy ligand, substituents on the triazole ring will point away from the semiconductor surface in case of the 1,5-regioisomer offering the installation of hydrophobic alkyl chains to increase the solubility of the dyes, suppress water-induced dye-desorption, and potentially reduce recombination reactions in the DSSC.[39,40]

RESULTS AND DISCUSSION

Synthesis. The alkyne building block 6-ethynyl-2,2′-bipyridine and 2,6-diethynylpyridine[41] were obtaind via a Sonogashira cross-coupling reaction. To ensure the selective formation of 1,5-disubstituted triazoles, $RuCp^*(PPh_3)_2Cl$ (Cp* = pentamethylcyclopentadienyl) was chosen as catalyst for the subsequent azide−alkyne cycloaddition[42−44] with *n*-octyl azide, which afforded the 1,2,3-triazole frameworks **5** and **6** in good yields (Scheme 1). Methylation of **6** was accomplished using Meerwein's reagent as reported previously.[25] In view of the wide scope of available azides and the potential to use substituted alkynyl-pyridine building blocks, modularly functionalized ligands are thus available.

The cyclometalated complexes **1a** and **1b** were obtained in good yields by converting ligand **5** with $[Ru^{II}(tpy)(MeCN)_3](PF_6)_2$ and $[Ru^{II}(tcmtpy)(MeCN)_3](PF_6)_2$ (tcmtpy = trimethyl-2,2′:6′,2″-terpyridine-4,4′,4″-tricarboxylate), respectively, under microwave irraditation in ethanol or DMF.[16,18] As a partial alkylation of the triazolide was already encountered under the acidic reaction conditions when alcohols were used as solvents, either 2,6-lutidine was added or DMF was used instead of the alcohol. Formation of **2a** and **2b** was achieved conveniently by alkylation of the respective 1,2,3-triazolide complexes **1a** and **1b** using methyl iodide.[45] The changes in the ^{13}C NMR spectral shifts of the ruthenium(II)-coordinated carbon atom upon alkylation were only marginal; however, the formation of the anticipated product was proven by 2D NMR techniques as well as mass spectrometry. Additionally, selective NOESY measurements were performed (see the SI), revealing a correlation between the α-CH_2 protons of the alkyl chain and the central pyridine ring, while no correlation was found for the methyl groups in line with the anticipated substitution pattern.

In contrast to the aforementioned 1,2,3-triazolylidene formation at the complex, the bis(triazolylidene) complex **3b** was synthesized via preparation of a silver(I) 1,2,3-triazolylidene complex and subsequent transmetalation using *cis*-$Ru(tcmtpy)(DMSO)Cl_2$, as reported for the synthesis of **3a** and derivatives thereof.[25,26] For the formation of the silver(I) precursor by reacting the triazolium salt **7** with Ag_2O, KBr had to be added to increase the reactivity of Ag_2O,[46] as the acidity of the alkyl-substituted triazolium salt is lower than that of previously used aryl-substituted analogues.[30,47] The saponification of the esters **1b**−**3b** was achieved in good yields by heating the corresponding complexes in $DMF/NEt_3/H_2O$ (3:1:1 *v*/*v*/*v*) according to literature protocols.[34,48,49]

Computational Methods. In order to gain a deeper insight into the photophysical and electrochemical properties of the complexes, density functional theory (DFT) and time-dependent (TD) DFT calculations have been carried out for the methyl-ester-substituted complexes. Octyl chains have been replaced by methyl groups (**1b′**−**3b′**) to shorten the computation time.

The relevant molecular orbitals, depicted in Table S1, reflect the electronic effects of the employed ligands. Due to the strong σ- and π-donating character of the anionic ligand of **1b′**, the HOMO is constituted of ruthenium d orbitals and triazolide π orbitals, while the LUMO is predominantly composed of tpy π^* orbitals. As a result of the electronic repulsion between the π orbitals of the triazolide and occupied metal d orbitals (π donation), the HOMO is strongly destabilized, which, in turn, leads to an increased π back-donation toward the tpy and, hence, the LUMO is destabilized as well, although to a lesser extent. Consequently, **1b′** features a relatively narrow HOMO−LUMO gap. In contrast, the HOMO of **2b′** is 0.6 eV lower in

dx.doi.org/10.1021/ic402702z | Inorg. Chem. 2014, 53, 2083−2095

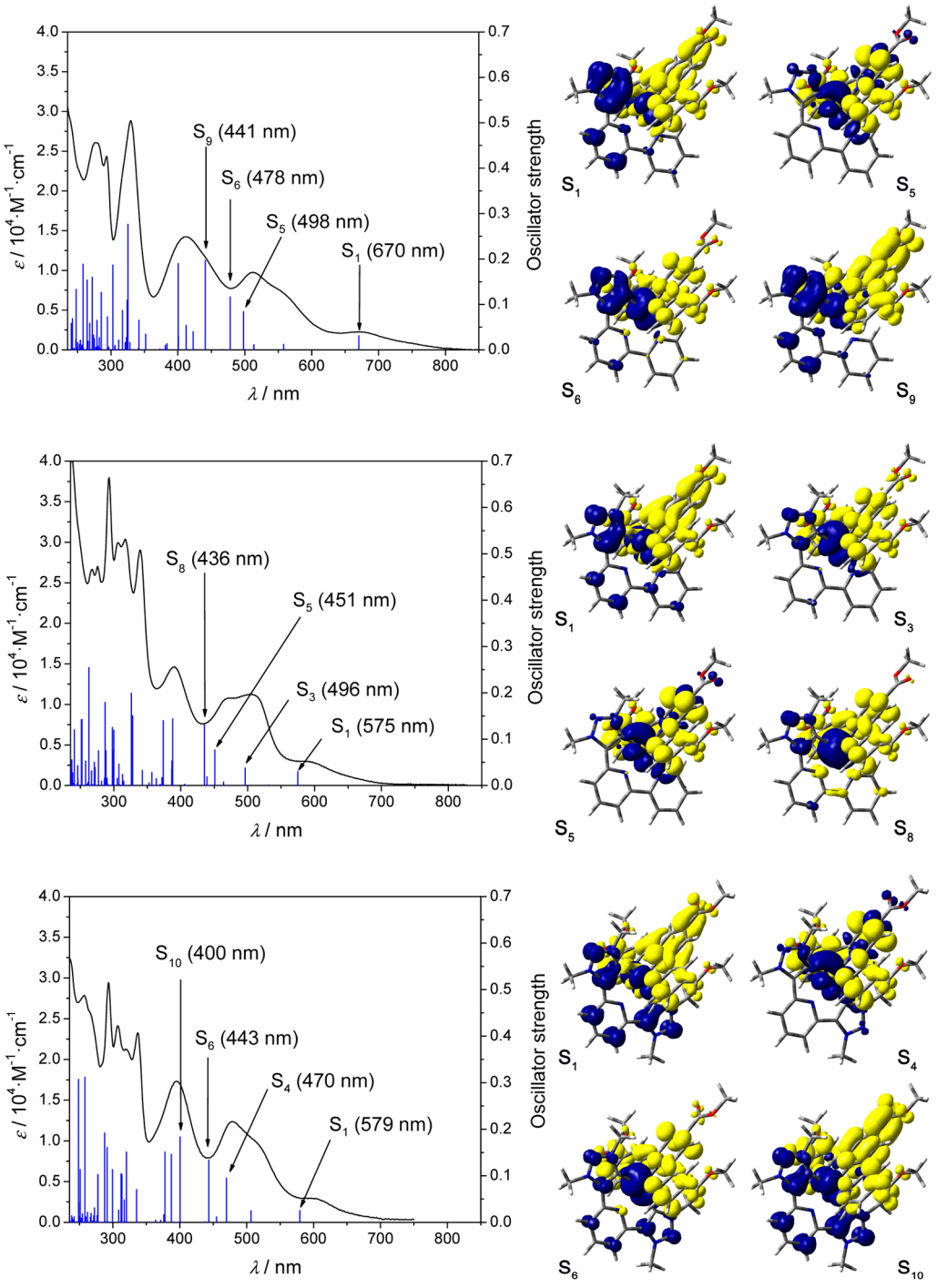

Figure 4. Calculated electronic singlet−singlet transitions and experimental UV−vis absorption spectra for the ester-substituted complexes (left, from top to bottom: **1b**′−**3b**′) and corresponding EDDM plots (right, blue = depletion of electron density, yellow = accumulation of electron density, isovalue = 0.001). Molecular orbitals involved in the transition are depicted in Table S1.

energy due to the moderate π-accepting character of the mesoionic carbene.[25] On account of the less electron-rich metal center, the destabilization of the tpy-based LUMO is also less pronounced resulting in a HOMO−LUMO gap of **2b**′ that is, all in all, 0.3 eV larger than for **1b**′. Introduction of a second 1,2,3-triazolylidene donor (**3b**′) further increases the σ donation and, thus, the HOMO and LUMO destabilization, although the energy gap remains constant.

Electron-density difference maps (EDDMs), which display the depletion and accumulation of electron density during an electronic transition, have been calculated for the relevant transitions in the visible-light region (Figure 4, Tables S2−4). Importantly, the calculated transitions are in good correlation with the experimental UV−vis spectra (vide infra). For **1b**′, the longest-wavelength transition involves a charge transfer from the HOMO, located on the ruthenium(II) center and the cyclometalating ligand, more precisely the triazolide ring, to the LUMO, which spreads over the tpy ligand. The corresponding transition is thus best described as a mixed metal-to-ligand charge transfer (MLCT) and ligand-to-ligand charge transfer

dx.doi.org/10.1021/ic402702z | Inorg. Chem. 2014, 53, 2083−2095

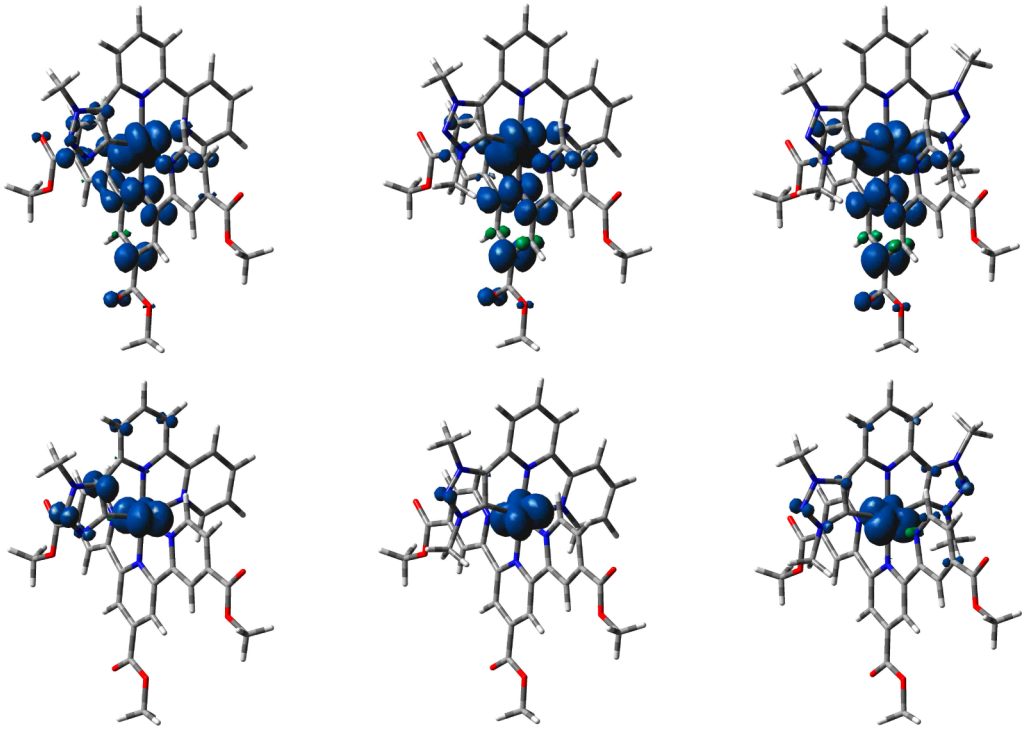

Figure 5. Spin-density plots (isovalue = 0.004) of the lowest-energy triplet excited state (top) and the singly oxidized GS (bottom) of the ester-substituted complexes (from left to right: **1b′**−**3b′**). Color code: Carbon, gray; hydrogen, white; nitrogen, blue; oxygen, red; ruthenium, cyan.

(LLCT), i.e., a metal-ligand-to-ligand charge-transfer (MLLCT) transition; however, the term MLCT is kept in the following (Figure 4, population of S_1).[50] The transitions at shorter wavelengths (between 350 and 600 nm) exhibit MLCT character with varying LLCT contributions (e.g., population of S_5, S_6, S_9). Certain transitions at ∼400 nm likewise show mixed MLCT and intraligand charge-transfer (ILCT) character involving the cyclometalating ligand, while absorption bands below 350 nm can be assigned to ligand-centered (LC) and metal-centered (MC) transitions. However, after internal conversion (IC), ultrafast intersystem crossing (ISC), and vibrational relaxation, the lowest-energy triplet excited-state is populated, which is expected to be a ^{3}MLCT featuring singly occupied molecular orbitals (SOMOs) located on the metal center/the anionic triazolide ring and the tpy ligand (vide infra). For the mesoionic carbene complexes **2b′** and **3b′**, the EDDM plots reveal a similar behavior as for **1b′**. The lowest-energy transitions involve a charge transfer from the HOMO, which is located on the carbene ligand and the metal, to the LUMO, located on the tpy ligand. Other transitions with high oscillator strengths in the visible region are of MLCT character involving lower occupied orbitals as well as higher unoccupied orbitals and are mostly directed toward the tpy ligand (Figure 4). Again, some MLCT transitions at shorter wavelengths are directed toward the carbene ligand and LC as well as MC transitions occur in the UV region.

Since we had previously encountered that the ISC is accompanied by a charge transfer from the tpy ligand to the carbene ligand in case of **3a**,[25] we also included a calculation of the spin-density distribution in the ^{3}MLCT for **1b′**−**3b′** (Figure 5). Owing to the stabilization of the π^* orbitals of the tpy ligand by the carboxymethyl groups, the initial electron transfer to the tpy is preserved in the lowest-energy ^{3}MLCT. With respect to application in DSSCs, the anchoring groups are therefore properly placed to allow for electron injection into TiO_2 (vide infra).

Furthermore, we calculated the spin-density distribution of the oxidized complexes (**1b′**$^+$−**3b′**$^+$, Figure 5), as this allows for an assessment of the localization of the electron hole remaining after the injection of an excited electron into the TiO_2. Similar to the HOMO distribution of **1b′** (Table S1), the cyclometalated ruthenium(III) complex **1b′**$^+$ shows significant spin density on the anionic triazolide ring, in contrast to the mesoionic carbene complexes. This finding is discussed below.

Photophysical Properties. The UV−vis absorption and emission spectra of the new complexes are depicted in Figures S12−S19, complemented with data for complex **3a**,[25] and the data is summarized in Table 1. In comparison to the parent homoleptic complex of tpy, $[Ru(tpy)_2](PF_6)_2$, the mesoionic carbene complexes **2a** and **3a** show MLCT maxima and absorption onsets at similar wavelengths but with lower extinction coefficients. Analogous behavior was reported recently for a tris(bidentate) ruthenium(II) complex featuring a 1,2,3-triazolylidene when compared to its polypyridyl counterpart $[Ru(bpy)_3](PF_6)_2$ (bpy = 2,2′-bipyridine).[51]

In contrast, the anionic triazolide of complex **1a** induces a bathochromic shift, in line with the DFT calculations (vide supra). In comparison to the analogous C^N^N-cyclometalated complex that features a phenyl anion as donor,[54,55] the bathochromic shift is less pronounced, which is expected based on the intrinsic lowering of the triazolide's electron donation by the ring nitrogen atoms.

The attachment of electron-withdrawing ester groups on the tpy (**1b**−**3b**) causes a bathochromic shift of the MLCT bands and absorption onsets due to the stabilization of tpy-based π^* orbitals. Furthermore, the ester groups increase the extinction coefficients (Table 1). However, the bathochromic shifts are

dx.doi.org/10.1021/ic402702z | Inorg. Chem. 2014, 53, 2083−2095

Table 1. Photophysical Data of the Complexes

complex	λ_{abs} /nm (ε/10^3 M^{-1} cm^{-1})[a−c]	λ_{em} /nm (λ_{exc} /nm); Φ_{PL}/%[b,d]	τ /ns[b,c]
$[Ru(tpy)_2](PF_6)_2$	520 (4.7), 475 (14.7), 308 (63.4), 274 (37.3)	–	0.21[e]
1a	619s (2.7), 505 (12.1), 386 (9.5), 316 (35.9)	730 (500); 0.2	35
1aH	542s (2.1), 476 (10.7), 400s (3.2), 310 (44.6)	648 (470); 1.8	47
2a	545s (2.7), 480 (10.4), 400 (4.5), 310 (40.4)	650 (478); 0.82	45
3a[f]	539 (3.0), 463 (10.5), 405 (5), 353 (9), 311 (28)	643 (463); 4.4	633
1b	672 (3.0), 556s (8.9), 512 (10.9), 414 (16.8), 329 (33.5)	∼ 800 (670); $<10^{-2}$	50
1bH	593 (2.8), 507 (10.8), 472 (10.2), 388 (13.9), 339 (26.4)	706 (510); 2.2	71
2b	593 (3.0), 503 (11.3), 471 (10.8), 391 (14.6), 339 (29.0)	703 (590); 3.0	133
3b	603 (3.0), 516s (9.7), 478 (12.3), 395 (17.3), 337 (23.3)	716 (600); 9.0	297
1c	626 (2.2),530s (8.4), 499 (10.6), 400 (10.1), 323 (29.4)[g]	736 (500)[g]	54[g]
2c	566 (2.9), 493 (11.7), 460s (10.5), 399 (6.2), 321 (35.1)[g]	671 (490)[g]	117[g]
3c	571 (2.6), 495 (10.5), 467 (11.6), 376 (8.7), 328 (26.4)[g]	674 (500)[g]	410, 306[g]

[a]s = shoulder. [b]Measured in MeCN unless stated otherwise. [c]Air-equilibrated solution. [d]Determined using $[Ru(dqp)_2](PF_6)_2$ in MeOH/EtOH 1:4 (ΦPL = 2.0%)[52] as reference; solutions were purged with N_2. [e]Taken from ref 53; measured in deaerated butyronitrile. [f]Taken from ref 25; measured in deaerated MeCN. [g]Measured in MeOH.

less pronounced for the complexes featuring free carboxylic acids (**1c**−**3c**) or TiO_2-anchored carboxylates (vide infra).

The E_{0-0} values follow the above-mentioned trends and are similar for the triazolylidene complexes, while they are significantly smaller for the 1,2,3-triazolide complexes (Table 2). Implications for the design of DSSCs thereof will be discussed later.

The cyclometalated ruthenium(II) complex **1a** is weakly emissive at room temperature in acetonitrile solution with slightly higher quantum yields (Φ_{PL} = 0.2%) than for ruthenium(II) complexes featuring cyclometalating phenyl rings.[16,54,55] The emission maximum at 723 nm is hypsochromically shifted relative to the emission maximum at about 800 nm observed for analogous ruthenium(II) complexes bearing a C^N^N-cyclometalating 6-phenyl-2,2′-bipyridine ligand,[54,55] which is again ascribed to the high degree of *aza* substitution within the 1,2,3-triazole ring lowering the GS destabilization. The excited-state lifetime was measured to be 35 ns, which is slightly shorter than for analogous ruthenium(II) complexes featuring a cyclometalating phenyl ring instead of the triazolide.[55] For **1b** and **1c**, prolonged excited-state lifetimes of 50 and 54 ns, respectively, were measured, which is attributed to a stabilization of the ^{3}MLCT and, thus, an increased energy separation between the ^{3}MLCT and the ^{3}MC. As reported earlier,[25−27] the introduction of 1,2,3-triazolylidenes as powerful σ donors enables a strong destabilization of the ^{3}MC relative to the ^{3}MLCT and, thus, the suppression of the radiationless deactivation via the ^{3}MC. In contrast to the cyclometalated complexes **1a** and **1b**, the GS and ^{3}MLCT destabilization is expected to be less pronounced due to the weaker π donation from the 1,2,3-triazolylidene. Consequently, the ^{3}MLCT−^{3}MC separation as well as the GS−^{3}MLCT gap is increased giving rise to longer-lived excited states and higher emission quantum yields. Indeed, **2a** and **2b** show excited-state lifetimes of 45 and 133 ns as well as phosphorescence quantum yields of 0.8% and 3.0%, respectively. Again, the electron-withdrawing ester groups further diminish the radiationless deactivation as they increase the ^{3}MLCT−^{3}MC energy separation by lowering the ^{3}MLCT energy. Even longer excited-state lifetimes (297 ns) and remarkably high phosphorescence quantum yields (9.0%) were measured for **3b** suggesting potential application in electroluminescence devices.[17,56−59] In comparison to the previously reported complex **3a**,[25] a shorter excited-state lifetime has been measured for **3b**, which is attributed to the use of air-equilibrated solvents for the

Table 2. Electrochemical Data of the Complexes

complex	$E_{1/2,ox}$ /V[a−c]	$E_{1/2,red}$/V[a−c]	E_{S^*} /V[a,d]	E_{0-0} /eV[b,e]
$[Ru(tpy)_2](PF_6)_2$	0.90[25]	−1.64[25]	–	–
1a	0.25	−1.93		1.88
1aH	0.67	–[f]	−1.44	2.11
2a	0.70	−1.75	−1.40	2.10
3a	0.60	−1.95	−1.49	2.09
1b	0.47	−1.51		1.67
1bH	0.86	–[f]	−1.02	1.88
2b	0.87	−1.35	−1.00	1.87
3b	0.73	−1.47	−1.12	1.85
1c	0.40 (1.03)[g]	–	−1.43 (−0.80)	1.83[h]
2c	0.84 (1.47)[g]	–	−1.13 (−0.50)	1.97[h]
3c	0.66 (1.29)[g]	–	−1.31 (−0.68)	1.97[h]
N749	0.16 (0.85)[i]	–	−1.42 (−0.73)	1.58[i]

[a]Referenced vs. Fc^+/Fc (vs. NHE). [b]Measured in MeCN solution unless stated otherwise. [c]Determined by cyclic voltammetry experiments using Bu_4NPF_6 as supporting electrolyte, unless stated otherwise; conversion to NHE scale by addition of 0.63 V[61] and 0.69 V[62] when the measurement was done in MeCN and DMF/MeOH (4:1 *v*/*v*), respectively. [d]Calculated using $E_{S^*} = E_{1/2,\,ox} - E_{0-0}$.[63] [e]Determined at the intersection of the absorption and emission spectra with the latter being normalized with respect to the lowest-energy absorption. [f]Could not be measured due to proton reduction with the added acid. [g]Determined by square-wave voltammetry with the complex-anchored TiO_2 anode as the working electrode immersed in MeCN containing Bu_4NPF_6 as supporting electrolyte; $OMFc^+$/OMFc was used as internal standard; conversion to Fc^+/Fc-scale by subtraction of 0.4 V and to NHE scale by addition of 0.23 V, i.e., *E* vs. Fc^+/Fc + 0.63 = *E* vs. NHE.[61,62,64] [h]Measured in MeOH solution. [i]Measured in DMF/MeOH (4:1 *v*/*v*) solution.

dx.doi.org/10.1021/ic402702z | *Inorg. Chem.* 2014, 53, 2083−2095

lifetime measurements. Also for the designated photosensitizers featuring free carboxylic acids, **2c** and **3c**, long excited-state lifetimes of 117 and 306 ns, respectively, have been measured in methanol solution despite the presence of oxygen in the solvent. Accordingly, oxygen exclusion is not required during the DSSC fabrication.

An interesting feature of the complexes **1a**−**1c** is the reversible switchability of the ligand's donor properties between the anionic triazolide and an *N*-protonated triazolide ring, i.e., a mesoionic 1,2,3-triazolylidene,[60] as exemplarily shown for **1a** in Figure 6. The optical properties of the protonated forms, **1aH**

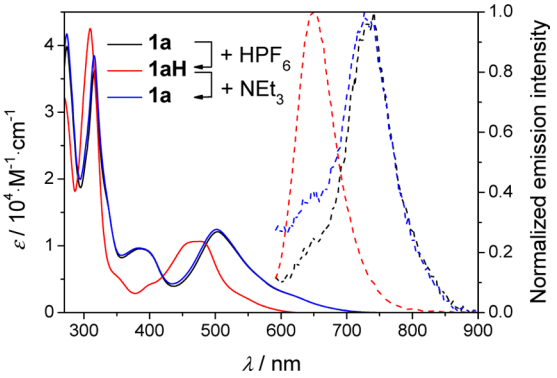

Figure 6. UV−vis spectral changes upon protonation and deprotonation of **1a** and **1aH**, respectively.

and **1bH**, resemble those of **2a** and **2b**, respectively (Table 1). In the case of **2b**, however, the lifetimes are still significantly longer than for the corresponding complex **1bH**.

Electrochemical Properties. The redox behavior of the presented ruthenium(II) complexes (Table 2) follows the electronic and structural trends as discussed for the computational results and the photophysical properties. Accordingly, the Ru(III)/Ru(II) redox potentials are the lowest for the complexes **1a**−**1c** (0.25, 0.47, and 0.40 V vs. Fc^+/Fc, respectively), intermediate for **3a**−**3c** (0.60, 0.73, and 0.66 V vs. Fc^+/Fc, respectively), and highest for **2a**−**2c** (0.70, 0.87, and 0.84 V vs. Fc^+/Fc, respectively), reflecting the electron donation by the anionic triazolide and the mesoionic triazolylidene donors. Importantly, the ruthenium-based redox process is fully reversible (Figure S20−S22). The tpy-based reduction follows the same trend: the more electron-rich the metal center, the more negative the redox potentials. This is attributed to a progressive destabilization of the tpy-based LUMO through π back-donation. In case of **3a**, however, the redox potential is even more negative than for **1a**, which might be rationalized by the close proximity between the mesityl moieties and the tpy plane giving rise to enhanced electronic repulsion upon tpy-based reduction. Similarly to the reduction process, the excited-state redox potentials (E_{S^*}) show a successive cathodic shift as the effective donor strength of the ligands increases (Table 2). Furthermore, the direct LUMO and indirect HOMO stabilization is stronger for the ester-functionalized complexes than for the complexes featuring carboxylic acid groups. Again, the electronic properties of the protonated cyclometalated complexes **1aH** and **1bH** resemble those of the carbene analogs **2a** and **2b**.

As a consequence of the strong σ donation from the 1,2,3-triazolylidenes and the strong σ and π donation from the 1,2,3-triazolide, the Ru(III)/Ru(II)-based redox process of **1a**−**3a** occurs at redox potentials that are significantly cathodically shifted relative to the parent $[Ru(tpy)_2]^{2+}$ (0.90 V vs. Fc^+/Fc).[25] Even for **2b**, featuring only a single 1,2,3-triazolylidene donor but three strongly electron-withdrawing −COOMe groups on the tpy ligand, the redox potential for the first oxidation is still slightly lower than for $[Ru(tpy)_2]^{2+}$. Also, for bis(tridentate) ruthenium(II) complexes featuring imidazol-2-ylidene-based ligands, the oxidation is facilitated relative to the tpy-analogous complexes.[24,65,66] On the other hand, a ruthenium(II) complex featuring a 2,6-bis(imidazol-2-ylidene)-pyridine and a 2,2′:6′,2″-terpyridine-4′-carboxylic acid ligand was reported to exhibit a metal-based redox process at 1.15 V vs. Fc^+/Fc,[67] which is remarkably dissimilar to the data measured for **3c** (0.66 V vs. Fc^+/Fc). Nonetheless, the higher donor strength of the 1,2,3-triazolylidene relative to imidazol-2-ylidene,[47,68] caused by the remote positioning of ring nitrogen atoms,[29,30,47,69] is expected to result in cathodically shifted ground- and excited-state redox potentials for the corresponding ruthenium(II) complexes. Accordingly, for a series of tris(bidentate) ruthenium(II) complexes containing either an imidazol-2-ylidene or a 1,2,3-triazolylidene, the latter showed a 140 mV less positive redox potential for the ruthenium-based oxidation process.[51] In comparison to **1a**, the C^N^N-coordinated ruthenium(II) complex featuring a cyclometalating phenyl ring shows a 100 mV lower Ru(III)/Ru(II)-based redox potential,[54] which reflects the weaker electron donation by the 1,2,3-triazolide.

Dye-Sensitized Solar Cells. In order to evaluate the performance of the presented triazolide and triazolylidene ruthenium(II) complexes in the DSSC, commercially available test cells with transparent TiO_2 anodes (12-μm-thick layer of 20 nm TiO_2 particles, 0.88 cm^2 active area) were used and assembled according to standard literature procedures.[70] A cell containing **N749** ($[Ru(Htctpy)(NCS)_3](NBu_4)_3$ with Htctpy = 2,2′:6′,2″-terpyridine-4′-carboxylic acid-4,4″-dicarboxylate)[71] as sensitizer and a I_3^-/I^--based electrolyte with a typical lithium iodide concentration of 0.1 M was included as internal standard.[72] In view of the less negative excited-state redox potentials of some of the new ruthenium(II) sensitizers (Figure 7) and in order to get an idea about their ability to achieve high incident photon-to-current efficiencies (IPCEs), an increased lithium iodide concentration of 1 M was used to lower the TiO_2 conduction band and, thereby, facilitate the electron injection

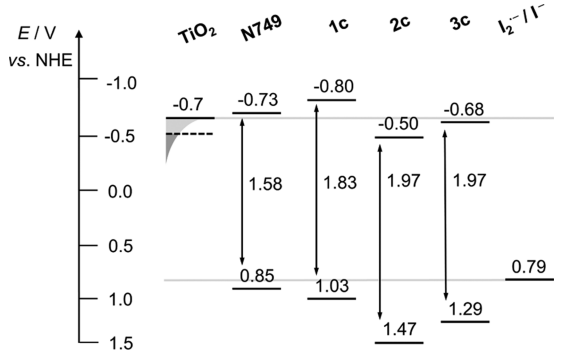

Figure 7. Comparison of the excited-state and ground-state redox potentials (values refer to the NHE scale, cf. Table 2) with the relevant redox potential of the electrolyte and the conduction band edge (solid line) as well as the appropriate position of the Fermi level (dashed line) of TiO_2.

dx.doi.org/10.1021/ic402702z | Inorg. Chem. 2014, 53, 2083−2095

into TiO_2 (vide infra).[31,73,74] However, the performance in the DSSC of **1c**–**3c** is clearly inferior to **N749** (Table 3).

Table 3. Selected DSSC Data for the Ru(II) Complexes Measured under AM1.5 Light Conditions

dye	$c(Li^+)$ /M	V_{OC} /V	J_{SC} /mAcm^{-2}	FF	PCE/%
1c	1	0.44	5.0	0.61	1.4
2c	1	0.38	1.9	0.61	0.5
3c	1	0.42	3.7	0.61	1.0
N749	0.1	0.69	11.6	0.62	5.1

Notably, the energy gaps of the presented sensitizers, which are larger than that of **N749** (Figure 7), cannot explain the significantly lower photocurrents on their own, as the integrated products of the absorbance of the dye-loaded TiO_2 films (see Figure S27) and the AM1.5 solar photon flux (with λ > 400 nm)[18,75] reveal overall light-harvesting capabilities relative to **N749** of 65%, 85%, and 77% for **1c**, **2c**, and **3c**, respectively.

In the case of **2c**, the excited-state redox potential (vide supra) lies considerably below the potential of the TiO_2 conduction band (Figure 7), which suppresses electron injection, in line with the low J_{sc} and IPCE values (Figures S28 and S29). In contrast, for **1c** and **3c**, injection problems should not be encountered due to the similar excited-state redox potentials of **1c**, **3c**, and **N749** (Figure 7), the prolonged lifetimes, particularly of **3c** (306 ns in methanol vs. 30 ns for **N749** in ethanol), and the high lithium concentration (1 M). Noteworthy, for osmium(II) sensitizers that feature a significantly lower excited-state redox potential than **N749**, high injection efficiencies had been achieved with a moderately increased lithium iodide concentration (0.6 M).[76] Inefficient dye regeneration might be another potential explanation. While it has been inferred that an electron hole on the dye that is exposed toward the electrolyte facilitates the dye regeneration by enabling an intimate contact with iodide,[86,88,89] for **2b**′ and **3b**′ (Figure 5, bottom), only marginal spin density is located on the ligand in the oxidized ground state according to the DFT calculations. Thus, although the positively shifted Ru(III)/Ru(II) redox potential provides a large regeneration driving force, the regeneration kinetics might be slow allowing for competitive backward electron transfer.[77,78]

Since not only the J_{sc} but also the V_{oc} values are quite low, even for the 1 M LiI additive, we suspect that an enhanced recombination of electrons in the TiO_2 conduction band with the oxidized dye is the main origin of the low PCE and IPCE values. Additionally, unfavorable interactions between the sensitizer and iodine could provoke recombination reactions with the electrolyte.[79−81] Furthermore, the long alkyl chains could also, in principle, slow down the regeneration kinetics; however, even lower PCEs have been observed with other ruthenium(II) carbene complexes devoid of alkyl chains,[27,67] while high PCEs have been achieved with sensitizers bearing even longer alkyl chains.[82,83]

In contrast to the carbene complexes, for the cyclometalated complex **1c**, a significant portion of the electron hole is located on the cyclometalating ligand (Figure 5). In line with the above mentioned argument, this is expected to facilitate dye regeneration. Indeed, **1c** shows the highest photocurrents despite its lower light-harvesting capabilities (vide supra). Still, the PCE and IPCE values of the cyclometalated complex **1c** are inferior to other photosensitizers featuring a carbanionic phenyl ring,[18,33,49,84,85] which may be attributed partly to a diminished electron injection on account of the less negative excited-state redox potential[86] and/or recombination reactions due to dye-iodine interaction.[79−81] Additionally, a partial lithium or proton coordination at the 3-nitrogen of the triazolide ring would render the electronic properties of **1c** similar to **2c** (vide supra).[60] While a protonation is unlikely due to the presence of 0.5 M 4-*tert*-butylpyridine in the electrolyte, and although UV–vis absorption and CV measurements with **1c** in acetonitrile solution containing either 1 M $LiClO_4$ or 1 M Bu_4NClO_4 did not indicate any interaction between **1c** and Li^+, it cannot be ruled out that the triazolide is affected in the working device.

Ultimately, as the sensitizers **1c** and **3c** do not show obvious molecular design drawbacks, we tentatively ascribe the comparably low PCE and IPCE values to unfavorable interactions between the sensitizer and the electrolyte and inefficient regeneration, respectively. Prospectively, **3c** might allow significantly improved IPCEs using electrolytes based on cobalt(III)/cobalt(II) polypyridyl complexes or ferrocenium/ferrocene, which would additionally allow the exploitation of the high Ru(III)/Ru(II) redox potential of the mesoionic carbene complex potentially leading to high V_{oc} values.[87−89]

CONCLUSION

A series of new bis(tridentate) ruthenium(II) complexes featuring ligands with anionic triazolide and mesoionic triazolylidene donors is presented. The σ and π donation from the triazolide carbanion is lowered in comparison to a phenyl anion due to the stabilization by three ring nitrogen atoms. The mesoionic carbenes are very strong σ donors but weak π donors resulting in a larger energy gap, more positive redox potentials, and a negligible ligand contribution to the HOMO in comparison to the triazolide complex. The 1,2,3-triazolide complexes can be reversibly switched to the corresponding 1,2,3-triazolylidene complexes by protonation. The emission of red light with relatively high photoluminescence quantum yields of the triazolylidene complexes suggests a potential application in electroluminescence devices. The presented ruthenium(II) complexes can be readily functionalized and show a broad absorption of visible light resulting in the formation of charge-separated excited states that feature relatively long lifetimes, in particular, in the case of the 1,2,3-triazolylidene complexes. These attractive photophysical properties suggest the application as photoredox catalysts or as photosensitizers for DSSC applications. The potential for the latter was investigated, but the achieved J_{sc} and V_{oc} values were relatively low, which is tentatively attributed to less efficient electron injection and/or dye regeneration.

EXPERIMENTAL SECTION

$[Ru^{II}(tpy)(MeCN)_3](PF_6)_2$, $[Ru^{II}(tcmtpy)(MeCN)_3](PF_6)_2$, 2,6-diethynylpyridine, and *n*-octyl azide were synthesized according to literature procedures.[16,41,90,91] Methanol was dried by distillation over magnesium and kept under nitrogen using standard Schlenk techniques. Anhydrous (99.8%) *N*,*N*-dimethylformamide (DMF) and $RuCp^*(PPh_3)_2Cl$ were purchased from Sigma-Aldrich. 4,4′,4″-Tricarboxymethyl-2,2′:6′,2″-terpyridine (tcmtpy) was purchased from hetcat. $[Ru(Htctpy)(NCS)_3](NBu_4)_3$ (**N749** or black dye; Htctpy = 2,2′:6′,2″-terpyridine-4′-carboxylic acid-4,4″-dicarboxylate) was purchased from Solaronix. All other chemicals were purchased from commercial suppliers and used as received. All reactions were performed in oven-dried flasks and were monitored by thin-layer chromatography (TLC) (silica gel on aluminum sheets with fluorescent dye F254, Merck KGaA). Microwave reactions were

dx.doi.org/10.1021/ic402702z | Inorg. Chem. 2014, 53, 2083−2095

carried out using a Biotage Initiator Microwave synthesizer. NMR spectra have been recorded on a Bruker AVANCE 250 MHz, AVANCE 300 MHz, or AVANCE 400 MHz instrument in deuterated solvents (euriso-top) at 25 °C. ^{1}H and ^{13}C resonances were assigned using appropriate 2D correlation spectra. Chemical shifts are reported in ppm using the solvent as internal standard. Matrix-assisted laser desorption-ionization time-of-flight (MALDI-TOF) mass spectra were obtained using an Ultraflex III TOF/TOF mass spectrometer with dithranol as matrix in reflector mode. High resolution electrospray ionization quadrupole time-of-flight mass spectrometry (ESI-Q-TOF MS) was performed on an ESI-Q-TOF-MS microTOF QII (Bruker Daltonics) mass spectrometer. UV/vis absorption spectra were recorded on a Perkin-Elmer Lambda 750 UV/vis spectrophotometer, emission spectra on a Jasco FP6500. Measurements were carried out using 10^{-6} M solutions of respective solvents (spectroscopy grade) in 1 cm quartz cuvettes or on dye-loaded, transparent TiO_2 anodes (12 μm thick, 0.88 cm^2 active area, see Cell Fabrication) at room temperature. Lifetime measurements were mostly obtained by time-correlated single-photon counting utliziling a Titan:Sapphire laser (Tsunami, Newport Spectra-Physics GmbH) as light source.[92] The repetition rate was set to 400 kHz (pulse generator, Model 3980) and the 500 nm pump beam created by a second harmonic generator from Newport Spectra-Physics GmbH. The emission is detected by a Becker & Hickel PMC-100-4 photon-counting module. Samples are prepared to yield an optical density of 0.1 at the excitation wavelength. Cyclic voltammetry measurements were performed on a Metrohm Autolab PGSTAT30 potentiostat with a standard three-electrode configuration using a graphite-disk working electrode, a platinum-rod auxiliary electrode, and a Ag/AgCl reference electrode; scan rates from 50 to 500 mV·s^{-1} were applied. The experiments were carried out in degassed solvents (spectroscopy grade) containing 0.1 M Bu_4NPF_6 salt (dried previously by heating at 110 °C and storing under vacuum). At the end of each measurement, ferrocene was added as an internal standard. All calculations are based on density functional theory (DFT). The geometries of the singlet ground state, the singly oxidized ground state, and the lowest triplet excited state have been optimized for all the ruthenium(II) complexes, presented herein. The hybrid functional B3LYP[93,94] has been selected in combination with the 6-31G* basis set for all atoms. To reproduce the measured absorption UV−vis spectrum, the lowest-lying 75 vertical singlet electronic excitation energies were calculated using time-dependent DFT (TD-DFT) at the S_0 optimized geometry. The TD-DFT calculations were performed in solution using acetonitrile as solvent with the polarization continuum model and with the same functional and basis set as in the optimizations.[95,96] All these calculations were performed with the *Gaussian09* program package.[97] The analysis of the EDDM calculations were performed by *GaussSum2.2*.[98] Electron density difference maps (density isovalue = 0.001), Kohn−Sham orbitals (MO isovalue = 0.04), and spin-density calculations (density isovalue = 0.004) were visualized by *GaussView5.0.8*.[97]

Synthesis of Ru(tcmtpy)(DMSO)Cl$_2$. $Ru(DMSO)_4Cl_2$ (1.2 g, 2.6 mmol), tcmtpy (391 mg, 0.96 mmol), and LiCl[99] (190 mg, 4.49 mmol) were suspended in 80 mL deaerated EtOH and the mixture was refluxed under a nitrogen atmosphere. After 5 h, the full conversion of tcmtpy was confirmed by TLC and the reaction mixture was allowed to cool to room temperature. The solvent was evaporated in vacuo and the remaining solid was suspended in H_2O, filtered, and washed with H_2O (3 × 3 mL), EtOH (2 × 3 mL), and Et_2O (3 × 3 mL) to yield 406 mg (0.62 mmol, 64%) of a purple solid. The product was stored under a nitrogen atmosphere in the fridge. ^{1}H NMR (300 MHz, DMSO-d$_6$) δ = 9.24 (d, J = 5.6 Hz, 2H, $H^{6,6''}$), 9.20 (s, 2H, $H^{3,3''}$), 9.17 (s, 2H, $H^{3',5'}$), 8.29 (d, J = 4.5 Hz, 2H, $H^{5,5''}$), 4.06 (s, 3H,C$^{4'}$−COOCH_3), 4.02 (s, 6H,C$^{4,4''}$−COOCH_3), 2.62−2.53 (m, 6H, DMSO-d$_6$) ppm; ^{13}C NMR (63 MHz, DMSO-d$_6$) δ = 164.5 (C$^{4'}$−COOMe), 164.2 (C$^{4,4''}$−$COOCH_3$), 160.1 ($C^{2,2''}$), 159.4 ($C^{2',6'}$), 153.8 ($C^{6,6''}$), 137.6 ($C^{4,4''}$), 133.7 (C^{4}), 127.1 ($C^{5,5''}$), 122.7 ($C^{3',5'}$), 122.3 ($C^{3,3''}$), 53.2 (C$^{4,4',4''}$−$COOCH_3$), 41.6 ppm.

Synthesis of 6-(Trimethylsilyl ethynyl)-2,2′-bipyridine. Under a nitrogen atmosphere, 6-bromo-2,2′-bipyridine (2 g, 8.51 mmol), $Pd(PPh_3)_4$ (479 mg, 0.41 mmol, 5 mol %), CuI (180 mg, 0.95 mmol, 11 mol %) were suspended in a mixture of dry and nitrogen-purged THF (35 mL) and diisopropylamine (4 mL). While stirring, trimethylsilylacetylene (2.5 mL, 17.87 mmol, 2 equiv) was added dropwise at room temperature. After stirring for 24 h at room temperature, additional trimethylsilylacetylene (1 mL) was added. After additional 96 h, the full conversion was confirmed by GC-MS and TLC. After addition of aq. EDTA (1 mL, 35%) and H_2O, the crude product was extracted with CH_2Cl_2 and subjected to column chromatography (silica, CH_2Cl_2/MeOH, 99:1 or alumina, CH_2Cl_2) to obtain 1.01 g (4.01 mmol, 47%) of a colorless solid. ^{1}H NMR (400 MHz, CD_2Cl_2) δ = 8.65 (dd, ^{3}J = 3.9, ^{4}J = 0.8 Hz, 1H, H^{6a}), 8.47−8.35 (m, 2H, $H^{3a,3a'}$), 7.90−7.74 (m, 2H, $H^{4a,4a'}$), 7.48 (d, ^{3}J = 7.7 Hz, 1H, $H^{5a'}$), 7.39−7.28 (m, 1H, H^{5a}), 0.33 (s, 9H) ppm; ^{13}C NMR (100 MHz, CD_2Cl_2) δ = 156.8 ($C^{2a'}$), 155.7 (C^{2a}), 149.5 ($C^{6a'}$), 142.7 ($C^{6a'}$), 137.4 ($C^{4a'}$), 137.3 (C^{4a}), 127.8 (C^{5a}), 124.4 ($C^{5a'}$), 121.4 (C^{3a}), 120.8 ($C^{3a'}$), 104.4 (C^{tert}), 94.5 (Si−C^{tert}), −0.2 ppm (Si−CH_3); MS (HR ESI-Q-TOF): calcd. for $C_{15}H_{16}N_2SiNa$ ([M + Na]$^+$): m/z = 275.0975; found: m/z = 275.1023.

Synthesis of 4. 6-(Trimethylsilyl ethynyl)-2,2′-bipyridine (1 g, 3.96 mmol) was dissolved in THF/MeOH (1:1, 100 mL) and the resulting solution was purged with nitrogen. The solution was stirred at room temperature under a nitrogen atmosphere and KF (460 mg, 7.92 mmol, 2 equiv) was added portionwise. The reaction mixture was stirred under light exclusion at room temperature. After 24 h, the full conversion was confirmed by TLC (alumina, n-hexane/CH_2Cl_2, 2:1) and all volatiles were evaporated in vacuo. After purification by column chromatography (silica, CH_2Cl_2/MeOH, 99:1), 600 mg (3.33 mmol, 84%) of a colorless solid were obtained. ^{1}H NMR (400 MHz, CD_2Cl_2) δ = 8.66 (d, ^{3}J = 4.1 Hz, 1H, H^{6a}), 8.43 (dd, ^{3}J = 8.0, ^{4}J = 2.1 Hz, 2H, $H^{3a,3a'}$), 7.88−7.77 (m, 2H, $H^{4a,4a'}$), 7.51 (dd, ^{3}J = 7.6, ^{4}J = 0.8 Hz, 1H, $H^{5a'}$), 7.38−7.29 (m, 1H, H^{5a}), 3.23 (s, 1H, C^{tert}CH) ppm; ^{13}C NMR (100 MHz, CD_2Cl_2) δ = 156.9 ($C^{2a'}$), 155.6 (C^{2a}), 149.5 (C^{6a}), 141.9 ($C^{6a'}$), 137.5 ($C^{4a'}$), 137.3 (C^{4a}), 127.9 (C^{5a}), 124.5 ($C^{5a'}$), 121.4 (C^{3a}), 121.2 ($C^{3a'}$), 83.3 (C^{tert}), 76.8 ppm (C^{tert}CH); MS (HR ESI-Q-TOF): calcd. for $C_{12}H_8N_2Na$ ([M + Na]$^+$): m/z = 203.058; found: m/z = 203.0618.

Synthesis of 5. **4** (79 mg, 0.44 mmol), n-octyl azide (150 mg, 0.97 mmol, 2.2 equiv), and $RuCp^*(PPh_3)_2Cl$ (7.3 mg, 0.009 mmol, 2 mol %) were suspended in dry and nitrogen-purged 1,4-dioxane (3.4 mL). Subsequently, the reaction mixture was heated to 60 °C for 3 h in the microwave reactor and the full conversion was confirmed by TLC (alumina, n-hexane/CH_2Cl_2, 1:1). The crude product mixture was subjected to column chromatography (silica, $CHCl_3$). After evaporation of the solvent, the remaining solid was suspended in hot n-hexane and filtered. The filtrate was concentrated and, after additional purification by column chromatography (alumina, n-hexane/CH_2Cl_2, 1:1) and removal of the solvent, 96.2 mg (0.29 mmol, 65%) of a yellow solid were obtained. ^{1}H NMR (250 MHz, CD_2Cl_2) δ = 8.70 (d, ^{3}J = 4.7 Hz, 1H, H^{6a}), 8.48 (d, ^{3}J = 8.0 Hz, 1H, $H^{3a'}$), 8.37 (d, ^{3}J = 8.0 Hz, 1H, H^{3a}), 8.01 (s, 1H, $H^{4a''}$), 7.95 (t, ^{3}J = 7.9 Hz, 1H, $H^{4a'}$), 7.86 (t, ^{3}J = 7.7 Hz, 1H, H^{4a}), 7.66 (d, ^{3}J = 7.8 Hz, 1H, $H^{5a'}$), 7.37 (t, ^{3}J = 6.17 Hz, 1H, H^{5a}), 4.96 (t, ^{3}J = 7.6 Hz, 2H, N−CH_2−), 2.05−1.85 (m, 2H, N−CH_2−CH_2−), 1.20 (s, 10H, −CH_2−), 0.83 (t, ^{3}J = 6.6 Hz, 3H, −CH_3) ppm; ^{13}C NMR (63 MHz, CD_2Cl_2) δ = 156.2 ($C^{2a'}$), 155.4 (C^{2a}), 149.3 (C^{6a}), 146.7 ($C^{6a'}$), 138.1 ($C^{4a'}$), 136.8 (C^{4a}), 135.5 ($C^{5a''}$), 133.5 ($C^{4a''}$), 124.1 (C^{5a}), 122.8 ($C^{5a'}$), 120.7 (C^{3a}), 120.4 ($C^{3a'}$), 50.1 (N−CH_2−), 31.7 (−CH_2−), 30.4 (−CH_2−), 29.1 (−CH_2−), 29.1 (−CH_2−), 26.5 (−CH_2−), 22.5 (−CH_2−), 13.8 (−CH_3) ppm; MS (HR ESI-Q-TOF): calcd. for $C_{20}H_{34}N_4O_7SNa$ ([M + Na]$^+$): m/z = 336.2183; found: m/z = 336.2165.

Synthesis of 6. n-Octyl azide (1.28 g, 8.24 mmol, 4.4 equiv), 2,6-diethynylpyridine (240 mg, 1.89 mmol), and $RuCp^*(PPh_3)_2Cl$ (30 mg, 0.04 mmol, 2 mol %) were dissolved in dry and nitrogen-purged 1,4-dioxane (9 mL). Subsequently, the reaction mixture was heated to 60 °C for 3 h in the microwave reactor and the full conversion of the alkyne was confirmed by TLC (alumina, CH_2Cl_2). The solvent was evaporated in vacuo and the crude product mixture was subjected to column chromatography (alumina, CH_2Cl_2/n-hexane, 3:1) to yield 665 mg (1.52 mmol, 81%) of a colorless solid. ^{1}H NMR (250 MHz, CD_2Cl_2) δ = 7.97 (s, 2H, $H^{4a,4a''}$), 7.96 (t, 1H, ^{3}J = 7.9 Hz, $H^{4a'}$), 7.62

dx.doi.org/10.1021/ic402702z | Inorg. Chem. 2014, 53, 2083−2095

(d, ^3J = 7.9 Hz, 2H, $H^{3a\prime,5a\prime}$), 4.75 (t, ^3J = 7.3 Hz, 4H, N−CH_2−), 1.94−1.67 (m, 4H, N−CH_2−CH_2−), 1.22 (d, ^3J = 23.3 Hz, 20H, −CH_2−), 0.84 (t, ^3J = 6.7 Hz, 6H, −CH_3) ppm; ^{13}C NMR (63 MHz, CD_2Cl_2) δ = 148.1 ($C^{2a\prime,6a\prime}$), 138.9 ($C^{4a\prime}$), 135.8 ($C^{5a,5a\prime\prime}$), 134.4 ($C^{4a,4a\prime\prime}$), 123.3 ($C^{3a\prime,5a\prime}$), 49.9 (N−CH_2−), 32.0 (−CH_2−), 30.6 (−CH_2−), 29.4 (−CH_2−), 29.3 (−CH_2−), 26.8 (−CH_2−), 22.9 (−CH_2−), 14.2 (−CH_3) ppm; MS (HR ESI-Q-TOF): calcd. for $C_{25}H_{39}N_7Na$ ([M + Na]$^+$): m/z = 460.3159; found: m/z = 460.3157; Elem. anal. calcd. for $C_{21}H_{31}N_7$ (437.62): C, 68.61%; H, 8.98%; N, 22.40%, found: C, 68.25%; H, 9.74%, N, 22.61%.

Synthesis of 7. In accordance with the literature,[25] **6** (319 mg, 0.73 mmol) was reacted with trimethyloxonium tetrafluoroborate (580 mg, 3.92 mmol, 5 equiv) in dry CH_2Cl_2 (6.8 mL) at room temperature for 48 h. The full conversion was confirmed by TLC (alumina, CH_2Cl_2) and MeOH (3 mL) was added dropwise to the reaction mixture. Subsequently, all volatiles were evaporated in vacuo and the resulting liquid was purified by column chromatography (alumina, MeCN/CH_2Cl_2, 3:1) to yield 423 mg (0.66 mmol, 90%) of a yellow oil. ^{1}H NMR (400 MHz, CD_2Cl_2) δ = 9.03 (s, 2H, $H^{4a,4a\prime\prime}$), 8.18 (d, ^3J = 8.9 Hz, 1H, $H^{4a\prime}$), 8.13−8.07 (m, 2H, $H^{3a\prime,5a\prime}$), 4.86 (t, ^3J = 7.3 Hz, 4H, N−CH_2−), 4.43 (s, 6H, N−CH_3), 2.08−1.86 (m, 4H, N−CH_2−CH_2−), 1.53−1.00 (m, 20H, −CH_2−), 0.86 (t, J = 6.9 Hz, 6H, −CH_3) ppm; ^{13}C NMR (101 MHz, CD_2Cl_2) δ = 143.9 ($C^{2a\prime,6a\prime}$), 141.2 ($C^{4a\prime}$), 140.3 ($C^{5a,5a\prime\prime}$), 132.0 ($C^{4a,4a\prime\prime}$), 127.7 ($C^{3a\prime,5a\prime}$), 54.4 (N−CH_2−), 54.2 (−CH_2−), 54.1 (−CH_2−), 53.8 (−CH_2−), 53.5 (−CH_2−), 53.3 (−CH_2−), 40.9 (−CH_2−), 32.0 (−CH_2−), 29.3 (−CH_2−), 29.3 (−CH_2−), 29.2 (−CH_2−), 26.5 (−CH_2−), 22.9 (−CH_2−), 14.2 (−CH_3) ppm; MS (HR ESI-Q-TOF): calcd. for $C_{27}H_{45}N_7BF_4$ ([M − BF_4]$^+$): m/z = 554.3765; found: m/z = 554.3755.

Synthesis of 8. **7** (234 mg, 0.37 mmol), KBr[46] (640 mg, 5.38 mmol, 15 equiv), and freshly prepared Ag_2O (700 mg, 3 mmol, 8 equiv) were suspended in dry and nitrogen-purged MeCN (15 mL). After stirring for 6 d under light exclusion at room temperature, the crude reaction mixture was diluted with dry CH_2Cl_2 and filtered over a Celite plug. Subsequently, all volatiles were evaporated in vacuo and the remaining solid was dissolved in CH_2Cl_2 and precipitated into *n*-hexane. The formed precipitate was filtered, washed with *n*-hexane, and rinsed with CH_2Cl_2. After evaporation of the solvent in vacuo, 264.4 mg (0.2 mmol, 55%) of a gold-brown solid were obtained. ^{1}H NMR (250 MHz, CD_2Cl_2) δ = 8.19−8.04 (m, 3H, $H^{3a\prime,4a\prime,5a\prime}$), 4.66 (t, ^3J = 7.3 Hz, 4H, N−CH_2−), 4.30 (s, 6H, N−CH_3), 1.81 (s, 4H, N−CH_2−CH_2−), 1.21 (d, J = 24.0 Hz, 20H, −CH_2−), 0.85 (t, J = 6.8 Hz, 6H, −CH_3) ppm; ^{13}C NMR (100 MHz, CD_2Cl_2) δ = 173.2, 172.2, 168.3, 148.2, 146.5, 143.6, 139.7, 125.8, 51.8, 43.6, 32.0, 29.9, 29.3, 29.1, 27.7, 26.56, 22.9, 14.2, ppm; MS (HR ESI-Q-TOF): calcd. for $C_{54}H_{86}Ag_2N_{14}$ ([dimer − 2$AgBr_2$]$^{2+}$): m/z = 573.2704; found: m/z = 573.2685; MS (ESI-TOF, negative mode): calcd. for $AgBr_2$ (counter-ion): m/z = 266.7397; found: m/z = 266.7403.

Synthesis of 1a. [Ru(tpy)(MeCN)$_3$] $(PF_6)_2$ (20 mg, 0.03 mmol), **5** (9 mg, 0.03 mmol), and 2,6-lutidine (15 μL, 0.129 mmol, 5 equiv) were dissolved in dry and nitrogen-purged MeOH (1 mL). Subsequently, the reaction mixture was heated to 130 °C for 30 min in the microwave reactor. After the full conversion of [Ru(tpy)-(MeCN)$_3$]$(PF_6)_2$ was confirmed by TLC (silica, MeCN/H_2O/aq KNO_3, 40:4:1), the crude product mixture was dropped into aq. NH_4PF_6. The formed precipitate was filtered, washed with H_2O, and rinsed with MeCN. After purification by column chromatography (alumina, CH_2Cl_2/MeCN, 4:1), 10 mg (0.01 mmol, 64%) of a violet solid were obtained. ^{1}H NMR (600 MHz, CD_3CN) δ = 8.55 (d, ^3J = 8.1 Hz, 2H, $H^{3\prime,5\prime}$), 8.41 (d, ^3J = 8.2 Hz, 1H, H^{3a}), 8.36 (d, ^3J = 8.1 Hz, 2H, $H^{3,3\prime\prime}$), 8.29 (d, ^3J = 7.9 Hz, 1H, $H^{5a\prime}$), 8.08 (t, ^3J = 8.0 Hz, 1H, $H^{4a\prime}$), 8.04 (t, ^3J = 8.1 Hz, 1H, $H^{4\prime}$), 8.01 (d, ^3J = 8.0 Hz, 1H, $H^{3a\prime}$), 7.83 (t, ^3J = 7.8 Hz, 1H, H^{4a}), 7.75 (t, ^3J = 7.9 Hz, 2H, $H^{4,4\prime\prime}$), 7.37 (d, ^3J = 5.3 Hz, 1H, H^{6a}), 7.35 (d, ^3J = 5.4 Hz, 2H, $H^{6,6\prime\prime}$), 7.10−7.03 (m, 3H, $H^{5,5\prime\prime,5a}$), 4.65 (t, ^3J = 7.1 Hz, 2H, N−CH_2−), 1.92−1.85 (m, 2H, N−CH_2−CH_2−), 1.42−1.13 (m, 10H, −CH_2−), 0.84 (t, J = 7.2 Hz, 3H, −CH_3) ppm; ^{13}C NMR (150 MHz, CD_3CN) δ = 177.8 (Ru−C), 158.3 ($C^{2,2\prime\prime}$), 156.9 ($C^{2a\prime}$), 156.8 (C^{2a}), 155.3 ($C^{2\prime,6\prime}$), 153.82 ($C^{6a\prime}$), 152.2 ($C^{6,6\prime\prime}$), 151.4 (C^{6a}), 140.8 ($C^{5a\prime\prime}$), 138.3 (C^{4a}), 136.4 ($C^{4a\prime}$), 136.2 ($C^{4,4\prime\prime}$), 131.1 ($C^{4\prime}$), 127.3 ($C^{5,5\prime\prime}$), 127.2 (C^{5a}), 124.4 (C^{3a}), 123.9 ($C^{3,3\prime\prime}$), 122.9 ($C^{3\prime,5\prime}$), 119.1 ($C^{3a\prime}$), 118.8 ($C^{5a\prime}$), 50.1 (N−CH_2−), 32.4 (−CH_2−), 30.7 (−CH_2−), 29.9 (−CH_2−), 29.7 (−CH_2−), 27.1 (−CH_2−), 23.3 (−CH_2−), 14.4 (−CH_3) ppm; MS (HR ESI-Q-TOF): calcd. for $C_{35}H_{35}N_8Ru$ ([M − PF_6]$^+$): m/z = 669.2031; found: m/z = 669.2016.

Synthesis of 2a. A microwave vial was charged with **1a** (6.3 mg, 0.01 mmol), MeI (1.5 μL, 0.024 mmol, 3 equiv), and dry $CHCl_3$ (0.6 mL). The vial was capped and heated to 70 °C for 24 h while stirring using an oil bath. The full conversion was confirmed by TLC (silica, MeCN/H_2O/aq.KNO_3, 40:4:1). All volatiles were evaporated in vacuo and the remaining solid was dissolved in MeCN, and dropped into aq. NH_4PF_6. The formed precipitate was filtered, washed with H_2O, and dried to yield 5.0 mg (0.005 mmol, 66%) of a red solid. ^{1}H NMR (600 MHz, CD_3CN) δ = 8.63 (d, ^3J = 8.1 Hz, 2H, $H^{3\prime,5\prime}$), 8.50 (d, ^3J = 7.4 Hz, 1H, $H^{5a\prime}$), 8.47 (d, ^3J = 8.1 Hz, 1H, H^{3a}), 8.41 (d, ^3J = 8.1 Hz, 2H, $H^{3,3\prime\prime}$), 8.29−8.21 (m, 3H, $H^{4\prime,3a\prime,4a\prime}$), 7.92 (t, ^3J = 7.8 Hz, 1H, H^{4a}), 7.87 (t, ^3J = 7.2 Hz, 2H, $H^{4,4\prime\prime}$), 7.40 (d, ^3J = 5.3 Hz, 1H, H^{6a}), 7.29 (d, ^3J = 5.3 Hz, 2H, $H^{6,6\prime\prime}$), 7.18 (d, ^3J = 6.5 Hz, 1H, H^{5a}), 7.12 (t, ^3J = 6.6 Hz, 2H, $H^{5,5\prime\prime}$), 4.76 (t, ^3J = 7.2 Hz, 2H, N−CH_2−), 3.06 (s, 3H, N−CH_3), 2.03−1.97 (m, 2H, N−CH_2−CH_2−),1.39−1.32 (m, 2H, N−CH_2−CH_2−CH_2), 1.32−1.16 (m, 8H, −CH_2−), 0.85 (t, ^3J = 7.1 Hz, 3H, −CH_3) ppm; ^{13}C NMR (75 MHz, CD_3CN) δ = 176.6 (Ru−C), 158.2 ($C^{2,2\prime\prime}$), 157.7 ($C^{2a\prime}$), 156.7 (C^{2a}), 155.73 ($C^{2\prime,6\prime}$), 153.2 ($C^{6,6\prime\prime}$), 151.3 (C^{6a}), 151.0 ($C^{6a\prime}$), 146.7 ($C^{5a\prime\prime}$), 139.2 (C^{4a}), 137.9 ($C^{4,4\prime}$), 137.1 ($C^{4a\prime}$), 134.8 ($C^{4\prime}$), 128.1 (C^{5a}), 128.0 ($C^{5,5\prime\prime}$), 125.1 (C^{3a}), 124.8 ($C^{3,3\prime\prime}$), 124.1 ($C^{3\prime,5\prime}$), 122.0 ($C^{5a\prime}$), 121.9 ($C^{3a\prime}$), 52.9 (N−CH_2−), 39.6 (−CH_2−), 32.3 (−CH_2−), 29.7 (−CH_2−), 29.5 (−CH_2−), 29.4 (−CH_2−), 26.7 (−CH_2−), 23.2 (−CH_2−), 14.3 (−CH_3) ppm; MS (HR ESI-Q-TOF): calcd. for $C_{36}H_{38}N_8Ru$ ([M − 2PF_6]$^{2+}$): m/z = 342.1122; found: m/z = 342.1131.

Synthesis of 1b. [Ru(tcmtpy)(MeCN)$_3$]$(PF_6)_2$ (62.5 mg, 0.07 mmol) and **5** (21.5 mg, 0.06) were dissolved in dry and nitrogen-purged DMF (2 mL). The reaction mixture was heated to 160 °C for 30 min in the microwave reactor. The full conversion of **5** was confirmed by TLC (alumina, CH_2Cl_2). The crude reaction mixture was precipitated in aq. NH_4PF_6, washed with H_2O, rinsed with MeCN and, subsequently, purified by column chromatography (silica, MeCN/H_2O/aq. KNO_3, 100:4:1). After anion exchange to PF_6^-, 21.3 mg (0.02 mmol, 34%) of a brown solid were obtained. ^{1}H NMR (400 MHz, CD_2Cl_2) δ = 9.12 (s, 2H, $H^{3\prime,5\prime}$), 8.90 (d, ^4J = 1.1 Hz, 2H, $H^{3,3\prime\prime}$), 8.47 (d, ^3J = 8.0 Hz, 1H, $H^{3a\prime}$), 8.43 (d, ^3J = 8.2 Hz, 1H, H^{3a}), 8.35 (t, ^3J = 8.1 Hz, 1H, $H^{4a\prime}$), 8.17 (d, ^3J = 8.0 Hz, 1H, $H^{5a\prime}$), 7.91 (dt, ^3J = 8.0, ^4J = 1.5 Hz, 1H, H^{4a}), 7.66 (dd, ^3J = 5.8, ^4J = 1.7 Hz, 2H, $H^{5,5\prime\prime}$), 7.50 (d, ^3J = 5.8 Hz, 2H, $H^{6,6\prime\prime}$), 7.21 (d, ^3J = 4.6 Hz, 1H, H^{6a}), 7.15 (t, ^3J = 6.5 Hz, 1H, H^{5a}), 4.79 (t, ^3J = 7.4 Hz, 2H, N−CH_2−), 4.17 (s, 3H, C$^{4\prime}$−COOCH_3), 3.96 (s, 6H, C$^{4,4\prime\prime}$−COOCH_3), 2.11−1.99 (m, 2H, N−CH_2−CH_2−), 1.58−1.09 (m, 10H, −CH_2−), 0.86 (t, ^3J = 6.9 Hz, 3H, −CH_3) ppm; ^{13}C NMR (100 MHz, CD_2Cl_2) δ = 173.2 (Ru−C), 164.7 (C$^{4\prime}$−COOMe), 164.0 (C$^{4,4\prime\prime}$−COOMe), 158.2 ($C^{2,2\prime\prime}$), 156.3 ($C^{2a\prime}$), 155.8 (C^{2a}), 155.1 ($C^{2\prime,6\prime}$), 152.5 ($C^{6,6\prime\prime}$), 150.5 ($C^{6a,6a\prime}$), 143.4 ($C^{5a\prime\prime}$), 139.0 (C^{4a}), 138.2 ($C^{4a\prime}$), 138.0 ($C^{4,4\prime\prime}$), 134.5 ($C^{4\prime}$), 127.8 (C^{5a}), 126.8 ($C^{5,5\prime\prime}$), 124.8 (C^{3a}), 123.0 ($C^{3,3\prime\prime}$), 122.8 ($C^{3\prime,5\prime}$), 120.9 ($C^{3a\prime}$), 120.7 ($C^{5a\prime}$), 53.7 (N−CH_2−), 53.5 (−CH_2−), 52.2 (−CH_2−), 32.0 (−CH_2−), 29.5 (−CH_2−), 29.4 (−CH_2−), 29.3 (−CH_2−), 26.7 (−CH_2−), 22.9 (−CH_2−), 14.2 (−CH_3) ppm; MS (HR ESI-Q-TOF): calcd. for $C_{41}H_{41}N_8O_6Ru$ ([M − PF_6]$^+$): m/z = 843.2198; found: m/z = 843.2204.

Synthesis of 2b. Following the same procedure as described for **2a**, **1b** (7.8 mg, 0.01 mmol) and MeI (1.5 μL, 0.02 mmol, 3 equiv) were reacted in dry $CHCl_3$ (0.6 mL) at 70 °C for 48 h. After anion exchange to PF_6^-, 6.5 mg (0.01 mmol, 71%) of a brown solid were obtained. ^{1}H NMR (400 MHz, CD_2Cl_2) δ = 9.22 (s, 2H, $H^{3\prime,5\prime}$), 8.96 (d, ^4J = 1.2 Hz, 2H, $H^{3,3\prime\prime}$), 8.51 (d, ^3J = 8.1 Hz, 1H, $H^{3a\prime}$), 8.47−8.36 (m, 2H, $H^{3a,4a\prime}$), 8.27 (d, ^3J = 8.0 Hz, 1H, $H^{5a\prime}$), 8.06−7.86 (m, 1H, H^{4a}), 7.76 (dd, ^3J = 5.8, ^4J = 1.6 Hz, 2H, $H^{5,5\prime\prime}$), 7.61 (d, ^3J = 5.8 Hz, 2H, $H^{6,6\prime\prime}$), 7.27 (d, ^3J = 4.7 Hz, 1H, H^{6a}), 7.23−7.13 (m, 1H, H^{5a}), 4.82 (t, ^3J = 7.5 Hz, 2H, N−CH_2−), 4.20 (s, 3H, C$^{4\prime}$−COOCH_3), 3.97 (s, 6H, C$^{4,4\prime\prime}$−COOCH_3), 3.08 (s, 3H), 2.17−2.02 (m, 2H, N−CH_2−CH_2−), 1.50−1.18 (m, 10H, −CH_2−), 0.86 (t, ^3J = 6.9 Hz, 3H, −CH_3) ppm; ^{13}C NMR (100 MHz, CD_2Cl_2) δ = 173.6 (Ru−C), 164.4

dx.doi.org/10.1021/ic402702z | Inorg. Chem. 2014, 53, 2083−2095

($C^{4'}$−COOMe), 163.9 ($C^{4,4''}$−COOMe), 157.4 ($C^{2,2''}$), 156.3 ($C^{2a'}$), 155.6 (C^{2a}), 155.4 ($C^{2',6'}$), 153.5 ($C^{6,6''}$), 150.8 (C^{6a}), 149.7 ($C^{6a'}$), 146.1 ($C^{5a''}$), 139.3 (C^{4a}), 138.7 ($C^{4a',4,4''}$), 135.4 ($C^{4'}$), 128.3 (C^{5a}), 127.8 ($C^{5,5''}$), 124.9 (C^{3a}), 123.4 ($C^{3,3''}$), 123.2 ($C^{3',5'}$), 122.2 ($C^{5a'}$), 121.9 ($C^{3a'}$), 54.0 (N−CH_2−), 53.8 (−CH_2−), 53.0 (−CH_2−), 39.4 (−CH_2−), 36.5 (−CH_2−), 32.0 (−CH_2−), 29.3 (−CH_2−), 29.2 (−CH_2−), 28.8 (−CH_2−), 26.1 (−CH_2−), 22.9 (−CH_2−), 14.2 (−CH_3) ppm; MS (HR ESI-Q-TOF): calcd. for $C_{42}H_{44}N_8O_6Ru$ ([M − $2PF_6$]$^{2+}$): m/z = 429.1214; found: m/z = 429.1203.

Synthesis of 3b. Under a nitrogen atmosphere, a microwave vial was charged with **8** (52 mg, 0.06 mmol), Ru(tcmtpy)(DMSO)Cl_2 (41 mg, 0.06 mmol), and dry and nitrogen-purged CH_2Cl_2 (9 mL). The vial was capped and heated to 70 °C for 24 h while stirring using an oil bath. The reaction mixture was allowed to cool to room temperature and the solvent was evaporated. The remaining solid was dissolved in MeCN, followed by the precipitation in aq. NH_4PF_6, filtration, washing with H_2O, and rinsing with MeCN. The crude product was subjected to column chromatography (silica, MeCN/H_2O/aq. KNO_3, 100:2:1) and the anion was exchanged to PF_6^- again. After precipitation into diethyl ether from a concentrated MeCN solution, filtration, washing with diethyl ether, rinsing with MeCN, and evaporation of all volatiles in vacuo, 13 mg (0.01 mmol, 21%) of a brown solid were obtained. ^{1}H NMR (400 MHz, CD_2Cl_2) δ = 9.16 (s, 2H, $H^{3',5'}$), 8.96 (d, ^4J = 1.1 Hz, 2H, $H^{3,3''}$), 8.32 (t, ^3J = 8.2 Hz, 1H, $H^{4a'}$), 8.01 (d, ^3J = 8.2 Hz, 2H, $H^{3a',5a'}$), 7.79 (dd, ^3J = 5.8, ^4J = 1.7 Hz, 2H, $H^{5,5''}$), 7.75 (d, ^3J = 5.8 Hz, 2H, $H^{6,6''}$), 4.77 (t, ^3J = 7.5 Hz, 4H, N−CH_2−), 4.19 (s, 3H, $C^{4'}$−COOCH_3), 3.99 (s, 6H, $C^{4,4''}$−COOCH_3), 3.00 (s, 6H, N−CH_3), 2.12−2.01 (m, 4H, N−CH_2−CH_2−), 1.48−1.19 (m, 20H, −CH_2−), 0.86 (t, ^3J = 6.9 Hz, 6H, −CH_3) ppm; ^{13}C NMR (100 MHz, CD_2Cl_2) δ = 179.7 (Ru−C), 164.7 ($C^{4'}$−COOMe), 164.2 ($C^{4,4''}$−COOMe), 156.4 ($C^{2,2''}$), 154.3 ($C^{2',6'}$), 154.0 ($C^{5,5''}$), 151.1 ($C^{2a',6a'}$), 145.8 ($C^{4a'}$), 139.3 ($C^{5a,5a''}$), 137.6 ($C^{4,4''}$), 132.8 ($C^{4'}$), 127.3 ($C^{6,6''}$), 122.9 ($C^{3,3''}$), 122.2 ($C^{3',5'}$), 119.8 ($C^{3a',5a'}$), 54.2 (N−CH_2−), 53.7 (−CH_2−), 52.8 (−CH_2−), 39.4 (−CH_2−), 32.0 (−CH_2−), 29.4 (−CH_2−), 29.2 (−CH_2−), 28.9 (−CH_2−), 26.7 (−CH_2−), 22.9 (−CH_2−), 14.2 (−CH_3) ppm; MS (HR ESI-Q-TOF): calcd. for $C_{48}H_{60}N_{10}O_6Ru$ ([M − $2PF_6$]$^{2+}$): m/z = 487.1871; found: m/z = 487.1848.

General Procedure for the Saponification of the Complexes 1−3b. According to the literature,[49] the ester-substituted complex was suspended in a DMF/NEt_3/H_2O (3:1:1, *v*/*v*/*v*, 2 mL) and heated to reflux for 24 to 48 h under a nitrogen atmosphere. After the full conversion was confirmed by MALDI-TOF MS, the solvents were evaporated in vacuo and the remaining solid was suspended in CH_2Cl_2. After collection of the solid using a centrifuge, the solvent was decanted and the remaining solvent was dried in vacuo.

Synthesis of 1c. 1b (21.3 mg, 0.022 mmol) was reacted for 48 h to yield 16.1 mg (0.017 mmol, 79%) of a black solid. ^{1}H NMR (400 MHz, CD_3CN) δ = 9.21 (s, 2H), 9.01 (s, 2H), 8.75−8.61 (m, 2H), 8.48−8.33 (m, 2H), 7.99 (t, ^3J = 8.9 Hz, 1H), 7.60 (d, ^3J = 5.6 Hz, 2H), 7.55 (d, ^3J = 4.1 Hz, 1H), 7.48 (d, ^3J = 5.6 Hz, 2H), 7.26 (t, ^3J = 5.7 Hz, 1H), 2.16−2.04 (m, 2H), 1.32 (s, 10H), 0.97−0.82 (m, 3H); MS (MALDI-TOF): calcd. for $C_{38}H_{35}N_8O_6Ru$ (M − PF_6]$^+$): m/z = 801.174; found: m/z = 801.252.

Synthesis of 2c. 2b (16 mg, 0.014 mmol) was reacted for 24 h to yield 11.4 mg (0.012 mmol, 85%) of a black solid. ^{1}H NMR (400 MHz, MeOD) δ = 9.33 (s, 2H), 9.08 (s, 2H), 8.77 (d, ^3J = 8.1 Hz, 1H), 8.70 (d, ^3J = 8.0 Hz, 1H), 8.53−8.39 (m, 2H), 8.02 (t, ^3J = 7.2 Hz, 1H), 7.68 (d, ^3J = 4.2 Hz, 2H), 7.59−7.51 (m, 3H), 7.28 (t, ^3J = 6.6 Hz, 1H), 3.20 (s, 3H), 2.19−2.02 (m, 2H), 1.52−1.18 (m, 10H), 0.88 (t, ^3J = 7.1 Hz, 3H). MS (MALDI-TOF): calcd. for $C_{39}H_{38}N_8O_6Ru$ ([M − $2PF_6$]$^+$): m/z = 816.196; found: m/z = 816.354.

Synthesis of 3c. 3b (20.6 mg, 0.016 mmol) was reacted for 48 h to yield 15.3 mg (0.014 mmol, 87%) of a deep brown solid. ^{1}H NMR (400 MHz, CD_3CN) δ = 9.25 (s, 2H), 9.05 (s, 2H), 8.32 (t, ^3J = 8.1 Hz, 1H), 8.23 (d, ^3J = 8.2 Hz, 2H), 7.66 (d, ^3J = 4.3 Hz, 2H), 7.60 (d, ^3J = 5.8 Hz, 2H), 3.15 (s, 6H), 2.15−2.03 (m, 4H), 1.51−1.17 (m, 20H), 0.88 (t, ^3J = 6.9 Hz, 6H); MS (MALDI-TOF): calcd. for $C_{45}H_{54}N_{10}O_6Ru$ ([M − $2PF_6$]$^+$): m/z = 932.327; found: m/z = 932.463.

Cell Fabrication. Photoanodes were prefabricated by Dyesol, Inc. (Australia) with a screenprintable TiO_2 paste (18-NRT, Dyesol). The active area of the TiO_2 electrode is 0.88 cm^2 with a thickness of 12 μm (18-NRT) on fluorine-doped tin-oxide (FTO; TEC15 (15 Ω cm^{-2})). TiO_2 substrates were treated with $TiCl_4$(aq) (0.05 M) at 70 °C for 30 min and subsequently rinsed with H_2O and EtOH and dried prior to heating. The electrodes were heated to 450 °C for 20 min under ambient atmosphere and allowed to cool to 80 °C before dipping into the dye solution. The anode was soaked overnight for 16 h in anhydrous methanol and ethanol containing ∼0.25 mM **1c−3c** and **N749**, respectively. The stained films were rinsed copiously with the solvent they were dipped in and subsequently dried. The cells were fabricated using a Pt-coated counter-electrode (FTO TEC-15 (15 Ω cm^{-2})) and sandwiched with a 30 μm Surlyn (Dupont) gasket by resistive heating. The acetonitrile-based electrolytes contained 0.1 M guanidinium thiocyanate (GuSCN), 0.5 M 4-*tert*-butylpyridine (TBP), 0.06 M iodine, 0.6 M 1,3-dimethylimidazolium iodide (DMII), and either 1 M (**1c−3c**) or 0.1 M (**N749**) LiI. The electrolyte was introduced to the void via vacuum backfilling through a hole in the counter electrode. The hole was sealed with an aluminum-backed Bynel foil (Dyesol). After sealing, silver bus bars were added to all cells.[70]

■ ASSOCIATED CONTENT

Ⓢ Supporting Information

Figures S1−S83: Additional computational, photophysical, and electrochemical data as well as NMR, ESI-TOF MS and MALDI-TOF MS spectra. This material is available free of charge via the Internet at http://pubs.acs.org.

■ AUTHOR INFORMATION

Corresponding Authors

*E-mail: cberling@chem.ubc.ca.
*E-mail: benjamin.dietzek@uni-jena.de.
*E-mail: ulrich.schubert@uni-jena.de.

Notes

The authors declare no competing financial interest.

■ ACKNOWLEDGMENTS

B.S. and C.F. are grateful to the Fonds der Chemischen Industrie for Ph.D. scholarships. B. D. is grateful to the Fonds der Chemischen Industrie for financial support. M. J. is grateful to the Carl Zeiss foundation for financial support. D.G.B. and C.P.B. are grateful to the Canadian Natural Science and Engineering Research Council, the Canadian Foundation for Innovation, and the Alfred P. Sloan Foundation for their support.

■ REFERENCES

(1) Prier, C. K.; Rankic, D. A.; MacMillan, D. W. C. *Chem. Rev.* **2013**, *113*, 5322.
(2) Tschierlei, S.; Karnahl, M.; Presselt, M.; Dietzek, B.; Guthmuller, J.; González, L.; Schmitt, M.; Rau, S.; Popp, J. *Angew. Chem., Int. Ed.* **2010**, *49*, 3981.
(3) Narayanam, J. M. R.; Stephenson, C. R. J. *Chem. Soc. Rev.* **2011**, *40*, 102.
(4) Zeitler, K. *Angew. Chem., Int. Ed.* **2009**, *48*, 9785.
(5) Tucker, J. W.; Stephenson, C. R. J. *J. Org. Chem.* **2012**, *77*, 1617.
(6) Alstrum-Acevedo, J. H.; Brennaman, M. K.; Meyer, T. J. *Inorg. Chem.* **2005**, *44*, 6802.
(7) Bomben, P. G.; Robson, K. C. D.; Koivisto, B. D.; Berlinguette, C. P. *Coord. Chem. Rev.* **2012**, *256*, 1438.
(8) Robson, K. C. D.; Bomben, P. G.; Berlinguette, C. P. *Dalton Trans.* **2012**, *41*, 7814.

(9) Yin, J.-F.; Velayudham, M.; Bhattacharya, D.; Lin, H.-C.; Lu, K.-L. *Coord. Chem. Rev.* **2012**, *256*, 3008.
(10) Juris, A.; Balzani, V.; Barigelletti, F.; Campagna, S.; Belser, P.; von Zelewsky, A. *Coord. Chem. Rev.* **1988**, *84*, 85.
(11) Sauvage, J.-P.; Collin, J.-P.; Chambron, J.-C.; Guillerez, S.; Coudret, C.; Balzani, V.; Barigelletti, F.; De Cola, L.; Flamigni, L. *Chem. Rev.* **1994**, *94*, 993.
(12) Borg, O. A.; Godinho, S. S. M. C.; Lundqvist, M. J.; Lunell, S.; Persson, P. *J. Phys. Chem. A* **2008**, *112*, 4470.
(13) Hammarström, L.; Johansson, O. *Coord. Chem. Rev.* **2010**, *254*, 2546.
(14) Medlycott, E. A.; Hanan, G. S. *Chem. Soc. Rev.* **2005**, *34*, 133.
(15) Medlycott, E. A.; Hanan, G. S. *Coord. Chem. Rev.* **2006**, *250*, 1763.
(16) Schulze, B.; Escudero, D.; Friebe, C.; Siebert, R.; Görls, H.; Sinn, S.; Thomas, M.; Mai, S.; Popp, J.; Dietzek, B.; González, L.; Schubert, U. S. *Chem.—Eur. J.* **2012**, *18*, 4010.
(17) Costa, R. D.; Ortí, E.; Bolink, H. J.; Monti, F.; Accorsi, G.; Armaroli, N. *Angew. Chem., Int. Ed.* **2012**, *51*, 8178.
(18) Schulze, B.; Brown, D. G.; Robson, K. C. D.; Friebe, C.; Jäger, M.; Birckner, E.; Berlinguette, C. P.; Schubert, U. S. *Chem.—Eur. J.* **2013**, *19*, 14171.
(19) Caspar, J. V.; Sullivan, B. P.; Kober, E. M.; Meyer, T. J. *Chem. Phys. Lett.* **1982**, *91*, 91.
(20) Wächtler, M.; Maiuri, M.; Brida, D.; Popp, J.; Rau, S.; Cerullo, G.; Dietzek, B. *ChemPhysChem* **2013**, *14*, 2973.
(21) Kalyanasundaram, K.; Nazeeruddin, M. K. *Chem. Phys. Lett.* **1992**, *193*, 292.
(22) Lees, A. J. *Chem. Rev.* **1987**, *87*, 711.
(23) Jayabharathi, J.; Thanikachalam, V.; Srinivasan, N.; Perumal, M. V. *Spectrochim. Acta, Part A* **2011**, *79*, 338.
(24) Son, S. U.; Park, K. H.; Lee, Y.-S.; Kim, B. Y.; Choi, C. H.; Lah, M. S.; Jang, Y. H.; Jang, D.-J.; Chung, Y. K. *Inorg. Chem.* **2004**, *43*, 6896.
(25) Schulze, B.; Escudero, D.; Friebe, C.; Siebert, R.; Görls, H.; Köhn, U.; Altuntas, E.; Baumgaertel, A.; Hager, M. D.; Winter, A.; Dietzek, B.; Popp, J.; González, L.; Schubert, U. S. *Chem.—Eur. J.* **2011**, *17*, 5494.
(26) Gentilini, D.; Gagliardi, A.; Auf der Maur, M.; Vesce, L.; D'Ercole, D.; Brown, T. M.; Reale, A.; Di Carlo, A. *J. Phys. Chem. C* **2012**, *116*, 1151.
(27) Brown, D. G.; Schauer, P. A.; Borau-Garcia, J.; Fancy, B. R.; Berlinguette, C. P. *J. Am. Chem. Soc.* **2013**, *135*, 1692.
(28) Note that the numeration of the 1,3-triazolylidene ring used in this article follows the priority of the *N*-substituents of the triazole, which differs from the usually employed synthetic route via the copper(I)-catalyzed azide−alkyne cycloaddition. To avoid ambiguities, we avoid an indication of the carbene position (C4 or C5) and only use the term 1,2,3-triazolylidene throughout this article except for the NMR assignment.
(29) Schuster, O.; Yang, L.; Raubenheimer, H. G.; Albrecht, M. *Chem. Rev.* **2009**, *109*, 3445.
(30) Schulze, B.; Schubert, U. S. *Chem. Soc. Rev.*, in press, DOI: 10.1039/c3cs60386e.
(31) Bai, Y.; Zhang, J.; Wang, Y.; Zhang, M.; Wang, P. *Langmuir* **2011**, *27*, 4749.
(32) Juozapavicius, M.; Kaucikas, M.; van Thor, J. J.; O'Regan, B. C. *J. Phys. Chem. C* **2013**, *117*, 116.
(33) Bessho, T.; Yoneda, E.; Yum, J.-H.; Guglielmi, M.; Tavernelli, I.; Imai, H.; Rothlisberger, U.; Nazeeruddin, M. K.; Grätzel, M. *J. Am. Chem. Soc.* **2009**, *131*, 5930.
(34) Bomben, P. G.; Thériault, K. D.; Berlinguette, C. P. *Eur. J. Inorg. Chem.* **2011**, 1806.
(35) Struthers, H.; Mindt, T. L.; Schibli, R. *Dalton Trans.* **2010**, *39*, 675.
(36) Crowley, J. D.; McMorran, D. A. In *Topics in Heterocyclic Chemistry: Click Triazoles*; Košmrlj, J., Ed.; Springer: Berlin, 2012; Vol. *28*, p 31.
(37) Zhang, L.; Chen, X.; Xue, P.; Sun, H. H. Y.; Williams, I. D.; Sharpless, K. B.; Fokin, V. V.; Jia, G. *J. Am. Chem. Soc.* **2005**, *127*, 15998.
(38) Liu, S.; Müller, P.; Takase, M. K.; Swager, T. M. *Inorg. Chem.* **2011**, *50*, 7598.
(39) Wang, M.; Moon, S.-J.; Zhou, D.; Le Formal, F.; Cevey-Ha, N.-L.; Humphry-Baker, R.; Grätzel, C.; Wang, P.; Zakeeruddin, S. M.; Grätzel, M. *Adv. Funct. Mater.* **2010**, *20*, 1821.
(40) Klein, C.; Nazeeruddin, M. K.; Di Censo, D.; Liska, P.; Grätzel, M. *Inorg. Chem.* **2004**, *43*, 4216.
(41) Shin, Y.; Fryxell, G. E.; Johnson, C. A., II; Haley, M. M. *Chem. Mater.* **2008**, *20*, 981.
(42) Lamberti, M.; Fortman, G. C.; Poater, A.; Broggi, J.; Slawin, A. M. Z.; Cavallo, L.; Nolan, S. P. *Organometallics* **2012**, *31*, 756.
(43) Boren, B. C.; Narayan, S.; Rasmussen, L. K.; Zhang, L.; Zhao, H.; Lin, Z.; Jia, G.; Fokin, V. V. *J. Am. Chem. Soc.* **2008**, *130*, 8923.
(44) Rasmussen, L. K.; Boren, B. C.; Fokin, V. V. *Org. Lett.* **2007**, *9*, 5337.
(45) Schuster, E. M.; Botoshansky, M.; Gandelman, M. *Dalton Trans.* **2011**, *40*, 8764.
(46) Keske, E. C.; Zenkina, O. V.; Wang, R.; Crudden, C. M. *Organometallics* **2012**, *31*, 456.
(47) Donnelly, K. F.; Petronilho, A.; Albrecht, M. *Chem. Commun.* **2013**, *49*, 1145.
(48) Wadman, S. H.; Kroon, J. M.; Bakker, K.; Havenith, R. W. A.; van Klink, G. P. M.; van Koten, G. *Organometallics* **2010**, *29*, 1569.
(49) Robson, K. C. D.; Koivisto, B. D.; Yella, A.; Sporinova, B.; Nazeeruddin, M. K.; Baumgartner, T.; Grätzel, M.; Berlinguette, C. P. *Inorg. Chem.* **2011**, *50*, 5494.
(50) Bomben, P. G.; Robson, K. C. D.; Sedach, P. A.; Berlinguette, C. P. *Inorg. Chem.* **2009**, *48*, 9631.
(51) Leigh, V.; Ghattas, W.; Lalrempuia, R.; Müller-Bunz, H.; Pryce, M. T.; Albrecht, M. *Inorg. Chem.* **2013**, *52*, 5395.
(52) Abrahamsson, M.; Jäger, M.; Österman, T.; Eriksson, L.; Persson, P.; Becker, H.-C.; Johansson, O.; Hammarström, L. *J. Am. Chem. Soc.* **2006**, *128*, 12616.
(53) Amini, A.; Harriman, A.; Mayeux, A. *Phys. Chem. Chem. Phys.* **2004**, *5*, 1157.
(54) Wadman, S. H.; Lutz, M.; Tooke, D. M.; Spek, A. L.; Hartl, F.; Havenith, R. W. A.; van Klink, G. P. M.; van Koten, G. *Inorg. Chem.* **2009**, *48*, 1887.
(55) Collin, J.-P.; Beley, M.; Sauvage, J.-P.; Barigelletti, F. *Inorg. Chim. Acta* **1991**, *186*, 91.
(56) Chou, P.-T.; Chi, Y. *Eur. J. Inorg. Chem.* **2006**, 3319.
(57) Armstrong, N. R.; Wightman, R. M.; Gross, E. M. *Annu. Rev. Phys. Chem.* **2001**, *52*, 391.
(58) Chou, P.-T.; Chi, Y. *Chem.—Eur. J.* **2007**, *13*, 380.
(59) Abruña, H. D. *J. Electrochem. Soc.* **1985**, *132*, 842.
(60) Álvarez, C. M.; García-Escudero, L. A.; García-Rodríguez, R.; Miguel, D. *Chem. Commun.* **2012**, *48*, 7209.
(61) Pavlishchuk, V. V.; Addison, A. W. *Inorg. Chim. Acta* **2000**, *298*, 97.
(62) Connelly, N. G.; Geiger, W. E. *Chem. Rev.* **1996**, *96*, 877.
(63) Hagfeldt, A.; Boschloo, G.; Sun, L.; Kloo, L.; Pettersson, H. *Chem. Rev.* **2010**, *110*, 6595.
(64) Bietti, M.; DiLabio, G. A.; Lanzalunga, O.; Salamone, M. *J. Org. Chem.* **2010**, *75*, 5875.
(65) Park, H.-J.; Yoo, S.; Shin, I.-S.; Chung, Y. K.; Kim, J. *Electroanalysis* **2013**, *25*, 1111.
(66) Park, H.-J.; Chung, Y. K. *Dalton Trans.* **2012**, *41*, 5678.
(67) Park, H.-J.; Kim, K. H.; Choi, S. Y.; Kim, H.-M.; Lee, W. I.; Kang, Y. K.; Chung, Y. K. *Inorg. Chem.* **2010**, *49*, 7340.
(68) Gusev, D. G. *Organometallics* **2009**, *28*, 6458.
(69) Crabtree, R. H. *Coord. Chem. Rev.* **2013**, *257*, 755.
(70) Bomben, P. G.; Borau-Garcia, J.; Berlinguette, C. P. *Chem. Commun.* **2012**, *48*, 5599.
(71) Nazeeruddin, M. K.; Péchy, P.; Renouard, T.; Zakeeruddin, S. M.; Humphry-Baker, R.; Comte, P.; Liska, P.; Cevey, L.; Costa, E.;

Shklover, V.; Spiccia, L.; Deacon, G. B.; Bignozzi, C. A.; Grätzel, M. *J. Am. Chem. Soc.* **2001**, *123*, 1613.
(72) Chiba, Y.; Islam, A.; Watanabe, Y.; Komiya, R.; Koide, N.; Han, L. *Jpn. J. Appl. Phys.* **2006**, *45*, L638.
(73) Jennings, J. R.; Wang, Q. *J. Phys. Chem. C* **2009**, *114*, 1715.
(74) Onicha, A. C.; Castellano, F. N. *J. Phys. Chem. C* **2010**, *114*, 6831.
(75) Hasan, K.; Zysman-Colman, E. *Inorg. Chem.* **2012**, *51*, 12560.
(76) Wu, K.-L.; Ho, S.-T.; Chou, C.-C.; Chang, Y.-C.; Pan, H.-A.; Chi, Y.; Chou, P.-T. *Angew. Chem., Int. Ed.* **2012**, *51*, 5642.
(77) Clifford, J. N.; Palomares, E.; Nazeeruddin, M. K.; Grätzel, M.; Durrant, J. R. *J. Phys. Chem. C* **2007**, *111*, 6561.
(78) Jennings, J. R.; Liu, Y.; Wang, Q. *J. Phys. Chem. C* **2011**, *115*, 15109.
(79) Li, X.; Reynal, A.; Barnes, P.; Humphry-Baker, R.; Zakeeruddin, S. M.; De Angelis, F.; O'Regan, B. C. *Phys. Chem. Chem. Phys.* **2012**, *14*, 15421.
(80) Reynal, A.; Forneli, A.; Martinez-Ferrero, E.; Sánchez-Díaz, A.; Vidal-Ferran, A.; O'Regan, B. C.; Palomares, E. *J. Am. Chem. Soc.* **2008**, *130*, 13558.
(81) Richards, C. E.; Anderson, A. Y.; Martiniani, S.; Law, C.; O'Regan, B. C. *J. Phys. Chem. Lett.* **2012**, *3*, 1980.
(82) Polander, L. E.; Yella, A.; Curchod, B. F. E.; Ashari Astani, N.; Teuscher, J.; Scopelliti, R.; Gao, P.; Mathew, S.; Moser, J.-E.; Tavernelli, I.; Rothlisberger, U.; Grätzel, M.; Nazeeruddin, M. K.; Frey, J. *Angew. Chem., Int. Ed.* **2013**, *52*, 8731.
(83) Mori, S. N.; Kubo, W.; Kanzaki, T.; Masaki, N.; Wada, Y.; Yanagida, S. *J. Phys. Chem. C* **2007**, *111*, 3522.
(84) Wadman, S. H.; Kroon, J. M.; Bakker, K.; Lutz, M.; Spek, A. L.; van Klink, G. P. M.; van Koten, G. *Chem. Commun* **2007**, 1907.
(85) Kisserwan, H.; Kamar, A.; Shoker, T.; Ghaddar, T. H. *Dalton Trans.* **2012**, *41*, 10643.
(86) Lin, H.-W.; Wang, Y.-S.; Huang, Z.-Y.; Lin, Y.-M.; Chen, C.-W.; Yang, S.-H.; Wu, K.-L.; Chi, Y.; Liu, S.-H.; Chou, P.-T. *Phys. Chem. Chem. Phys.* **2012**, *14*, 14190.
(87) Hamann, T. W. *Dalton Trans.* **2012**, *41*, 3111.
(88) Ondersma, J. W.; Hamann, T. W. *Coord. Chem. Rev.* **2013**, *257*, 1533.
(89) Daeneke, T.; Mozer, A. J.; Uemura, Y.; Makuta, S.; Fekete, M.; Tachibana, Y.; Koumura, N.; Bach, U.; Spiccia, L. *J. Am. Chem. Soc.* **2012**, *134*, 16925.
(90) Alvarez, S. G.; Alvarez, M. T. *Synthesis* **1997**, 413.
(91) Park, S. H. *Bull. Korean Chem. Soc.* **2003**, *24*, 253.
(92) Siebert, R.; Hunger, C.; Guthmuller, J.; Schlütter, F.; Winter, A.; Schubert, U. S.; González, L.; Dietzek, B.; Popp, J. *J. Phys. Chem. C* **2011**, *115*, 12677.
(93) Becke, A. D. *J. Chem. Phys.* **1993**, *98*, 5648.
(94) Lee, C.; Yang, W.; Parr, R. G. *Phys. Rev. B* **1988**, *37*, 785.
(95) Mennucci, B.; Tomasi, J. *J. Chem. Phys.* **1997**, *106*, 5151.
(96) Cossi, M.; Barone, V.; Mennucci, B.; Tomasi, J. *Chem. Phys. Lett.* **1998**, *286*, 253.
(97) Frisch, M. J.; Trucks, G. W.; Schlegel, H. B.; Scuseria, G. E.; Robb, M. A.; Cheeseman, J. R.; Scalmani, G.; Barone, V.; Mennucci, B.; Petersson, G. A.; Nakatsuji, H.; Caricato, M.; Li, X.; Hratchian, H. P.; Izmaylov, A. F.; Bloino, J.; Zheng, G.; Sonnenberg, J. L.; Hada, M.; Ehara, M.; Toyota, K.; Fukuda, R.; Hasegawa, J.; Ishida, M.; Nakajima, T.; Honda, Y.; Kitao, O.; Nakai, H.; Vreven, T.; Montgomery, J. A.; Peralta, J. E.; Ogliaro, F.; Bearpark, M.; Heyd, J. J.; Brothers, E.; Kudin, K. N.; Staroverov, V. N.; Kobayashi, R.; Normand, J.; Raghavachari, K.; Rendell, A.; Burant, J. C.; Iyengar, S. S.; Tomasi, J.; Cossi, M.; Rega, N.; Millam, J. M.; Klene, M.; Knox, J. E.; Cross, J. B.; Bakken, V.; Adamo, C.; Jaramillo, J.; Gomperts, R.; Stratmann, R. E.; Yazyev, O.; Austin, A. J.; Cammi, R.; Pomelli, C.; Ochterski, J. W.; Martin, R. L.; Morokuma, K.; Zakrzewski, V. G.; Voth, G. A.; Salvador, P.; Dannenberg, J. J.; Dapprich, S.; Daniels, A. D.; Foresman, J. B.; Ortiz, J. V.; Cioslowski, J.; Fox, D. J., *Gaussian 09*, Revision B.01; Gaussian Inc., Wallingford, CT, 2009.
(98) O'Boyle, N. M.; Tenderholt, A. L.; Langner, K. M. *J. Comput. Chem.* **2008**, *29*, 839.
(99) Wolpher, H.; Sinha, S.; Pan, J.; Johansson, A.; Lundqvist, M. J.; Persson, P.; Lomoth, R.; Bergquist, J.; Sun, L.; Sundström, V.; Åkermark, B.; Polívka, T. *Inorg. Chem.* **2007**, *46*, 638.